We thank the anonymous Reviewer for his/her encouraging comments. The Reviewer's suggestions were helpful and helped us to improve the quality of our manuscript. Below we give detailed answers to the general and technical comments. The Reviewer comments are *in italics* **and our reply** in blue standard text**.**

This manuscript reports the viscosity transition of α-pinene SOA generated during the CLOUD experiments at CERN at different temperatures using an optical method with a depolarization instrument. The method based on the different depolarizing properties of spherical and non-spherical shape of particles. The manuscript provides information of transition, which was defined as viscosity transition, from non-spherical to spherical shape when increasing RH (particles taking up water vapor). This study demonstrated an optical method that could be applied for the chamber studies on the phase transition of particles. The experimental methods are valid and the scientific approach and discussion are sound. The paper is well written and organized. I recommend it for publication with minor revision. Please see the following comments that the authors may want to consider in the revision.

General comment:

1, Previous studies as mentioned by the authors often have a definition based on physical properties, such as viscosity, for different phases, for example, liquid, viscosity < 100 Pa s. The definition of viscosity transition here in this manuscript is not very clear, the transition from non-spherical shape to spherical means transition from solid/semi- solid to liquid or solid to semi-solid? Spherical shape does not mean the particle is in liquid state. It is suggested to provide the clear definition of the viscosity-transition. The definition of viscosity-transition-RH is placed in the later part of the manuscript, P28594 line 16. The way it is defined is not really quantitatively; can "decrease significantly" and "reached a constant level" be quantitatively defined? I suggested make these definitions at the early part of the paper and indicate that these are instrumental defined, unless physical means/values are provided associated with this viscosity-transition for definition.

We agree with the Reviewer that in our case the change in the depolarisation properties does not necessary imply that the particles are liquid after the transition. Also, we do not directly measure the viscosity of the particles, but their shape. Thus, our viscosity-transitions as it was described cannot be related to any specific change in the viscosity. We can only estimate the viscosity of the particles based on previous studies (as suggested by the Reviewer) or based on the relaxation timescales (please see the answers below). In the revised manuscript we label the viscosity transition as viscosity/shape-transition, similar to Kidd et al. (2014). We hope that this illustrates the fact that the assumed change in the viscosity is based on the direct observation of the shape change. We define this term already in the Introduction and highlight that this transition is instrumental defined: "*We define an instrumental-based viscosity/shape-transition RH that describes the RH value, where the particles were observed to be spherical or isotropic according to our method.*" (p28580, line 13, old manuscript version).

Furthermore, to clearly state that our method can only detect the viscous state, but not measure the viscosity of the particles, several modification were made. Also any statements that the particle would be liquid after the measured viscosity/shape-transition were removed. These modifications include:

1. In the abstract, we modified lines 6-8: "*we deployed a new in-situ optical method to detect the viscous state of alpha-pinene SOA particles and measured their transition from the amorphous highly viscous state to states of lower viscosity*" and removed the word liquid in line 10.

2. Chapter 4.5: we added “or low-viscous” next to liquid at page 28594, line 25 (old manuscript version).
3. We added at the end of the first paragraph in conclusions that the method presented here does not provide a direct measure of viscosity: “*although the viscosity of the SOA particles cannot be directly determined from our measurements.*”

2, P28595, Line 8-23, as mentioned above the definition of viscosity transition is not clear, RHg indicates the transition from solid to semisolid, caution is needed when compare the viscosity-transition RH with RHg as authors also mentioned that the viscosity- transition RH is different from RHg. If I understand it correctly, most likely the viscosity- transition RH will be higher than RHg (how much higher depending on the definition of viscosity-transition RH). Line 18-19, it is lacking of logic here for reasoning the comparison with RHg, the transition timescale and atmospheric processes are the dynamic factors, they may affect the viscosity-transition RH measured in the chamber, but not the reasons for the comparison. Why the viscosity-transition RH is more relevant for atmospheric processes? P 28597, line 11-12, why it is directly relevant for GLASSY Transition of SOA, isn’t this conflict with the statement in P28595, line 8-11.

We agree with the Reviewer and removed this paragraph. It is more suitable to estimate the viscosity in our case and compare our results to previous studies as suggested by the Reviewer. A new paragraph was added (please see the Author's reply below) that better discusses the physical meaning of our viscosity/shape-transition.

3, It is recommended to calculate or estimation the viscosity based on the transition time, particle size changes with additional assumptions. Based on these data it may be possible to estimate the viscosity of the particles or at least the changes of viscosity during the transition. There are a few more studies that maybe useful. Kidd et al (2014) provided viscosity information for a-pinene SOA generated at different RH, Wang et al (2015) estimated the viscosity of a-pinene SOA as a function of temperature and RH, Song et al (2015) summarized a nice set of the viscosity data for a-pinene SOA from previous studies for comparison.

We estimated the viscosity during the transition based on the transition time and the size of the primary particle using the procedure described in Pajunoja et al., (2014). This leads to an estimation of viscosity of 10^7. We compared this viscosity value to observations listed by the Reviewer. However, the problem with comparing or relating to viscosity values from previous studies is that the studies are usually conducted at room temperatures. Therefore, the RH dependency of viscosity may not be trivially linked to our observations.

Consequently, a new paragraph was added to the chapter 4.5. “*As explained above, our method does not directly measure the change in the viscosity but provides the critical RH, where the water uptake is significantly enhanced and the particles start to relax rapidly due to the change in their viscosity. During this process the viscosity changes of the α-pinene SOA particles are not limited by diffusion on water into the particles as the assumed water diffusion timescales can be expected to be in the order of seconds (Price et al., 2015; Lienhard et al., 2015). We can now use the observed relaxation time (of the order of 10 minutes) to provide a rough estimate of the viscosity of the α-pinene SOA particles during their viscosity/shape-transition. However, it has to be kept in mind that the particle viscosity and the relaxation timescale are affected by the constant increase in the chamber RH by about 0.5% per minute, which increases the uncertainty of our estimate.*

For the estimation of the particle viscosity, we used the method described in Pajunoja et al. (2014). We can assume a primary particle size of 400 nm in an SOA aggregate and a surface tension of 35 mN/m (Pajunoja et al., 2014). With these numbers we get an estimated viscosity of 107 Pas. This *value describes the viscosity during the viscosity/shape-transition period. Previous studies (e.g. Renbaum-Wolff et al., 2013; Bateman et al., 2014; Kidd et al. (2014); Pajunoja et al., 2014) have studied the viscosity of α-pinene SOA particles at room temperatures. The studies have found that α-pinene SOA particles are generally in aqueous state already at RH> 70% (Song et al. (2014)). At colder temperatures we can expect the transition from viscous to aqueous state is shifted to higher RH (Wang et al. (2015)). As the measured viscosity/shape-transitions generally took place at RH< 70% the comparison with literature would suggest that albeit our SOA particles were spherical, they probably were not in aqueous state after the transition. Therefore, our measured viscosity/shape-transition would describe the change in the viscosity within a semi-solid material."*

Technical comments:

1, P28577, line 6, please provide full description of "CLOUD" and "CERN"

We added the full descriptions of these acronyms: "*In the CLOUD (Cosmics Leaving Outdoor Droplets) experiment at CERN (The European Organisation for Nuclear Research), we deployed...*".

2, P28578, line 25-27, please provide references for this statement

We added the reference Zhang et al., 2015.

3, P28582, line 10-12, please justify the assumption or provide references

There are several studies that have tried to retrieve the real refractive index of SOA particles (e.g. Schnaiter et al., 2005; Redmond and Thompson, 2011; Kim et al., 2010). However, most of these studies are performed at room temperatures and, where the SOA particles were likely in aqueous state. The reported refractive indexes for alpha-pinene SOA vary between 1.4-1.6. Furthermore, Kim et al. reported hat: "aerosol mass concentration, oxidation chemistry, temperature, and aerosol aging may all influence the refractive index". However, to our knowledge studies of the refractive index of viscous SOA particles have not yet been conducted. Therefore, we have to assume our refractive index and the best way to do this is to assume the refractive index of non-viscous alpha-pinene SOA.

The purpose for the modeling is to evaluate the magnitude of the depolarisation ratio and to show that small deviations from the spherical shape can induce measurable depolarisation. As the results are more qualitative than quantitative we don't see that the uncertainty in the refractive index will effect the main conclusions drawn from the modeling.

We removed the assumption that the Reviewer was referring to and modified the sentence in the lines 10-12 as follows: "*The refractive index of alpha-pinene SOA at near room temperatures has been shown to vary between 1.4 and 1.6 (Schnaiter et al., (2005); Kim et al., (2010); Redmond and Thompson, (2011)). As we do not have the information on the refractive index of viscous alpha-pinene SOA particles, we assumed in the modeling study a refractive index of 1.5+0i after Schnaiter et al., (2005).*"

4, P28585-28586, provide the full description of SMPS, CPC, ApicT etc.

We added the full description for Scattering Mobility Particle Sizer (SMPS), Condensation Particle Counter (CPC) and APicT (AIDA PCI in-cloud TDL).

5, P28586, What is the pressure in chamber during the experiments?

The chamber was always 5 mbar overpressure compared to atmospheric pressure. We added the following sentence to the second paragraph in section 3.2.2: "*The chamber was kept at 5 mbar overpressure to avoid under-pressure in the sampling instruments.*"

6, P28593, line 19-23, what do you mean "particle hardness"?

By hardness we mean the ability to resist the deliquescence (higher deliquescence point). To avoid confusion, we removed the word "hardness" and modified the lines 19-23 as follows: "*The O/C ratio affects the particle deliquescence point; in the case of alpha-pinene SOA particles, we can expect the deliquescence point to be at higher temperatures with increasing O/C ratio (Berkemeier et al., 2014).*"

7, P28595, line 1, as mentioned above, the viscosity-transition RH is not quantitatively defined, is it possible that the observed wider transition RH is due to the arbitrally defined gray area as shown in Figure 4? If consider the uncertainty of RH as described in P28586 (7-13%), there is no significantly wider RH ranges as shown in Table 1. There may be one only considerable larger range is for -38 degree C (› 10%) as compared to 5-7% for higher temp.

The Reviewer is correct, when pointing out that we did not take into account the uncertainty range of the RH measurements. The measured partial water vapor pressure is always below 100 Pa, so we have an uncertainty of 13% at each temperature. When taking this into account, we cannot claim that the larger RH range in the measurements would not be due to measurement uncertainty. Therefore, we removed the second conclusion and the discussion related to it.

However, we disagree that the viscosity-transition is not quantitatively defined. The grey areas were not selected arbitrarily, but are based on clear changes in the depolarisation signal.

8, P28595, line 3, in Table 1, the viscosity-transition RH values are shown in ranges. it is not convincing that viscosity-transition RH has linear dependency of temp. Please provide fitting data or supporting information for this statement.

The near linear temperature dependency of the viscosity-transition is based on the measured transition RH, i.e. the RH value, where the particles appeared spherical according to our measurements (the highest RH in the range). A linear fit could be performed to the data points with a slope of -6.3 and an offset of 284. However, as we measure the viscosity-transition that is somewhat different than the glass-transition in Koop et al. (2011), we do not wish to provide a linear fit to the data, as the Reviewer pointed out. We modified the sentence on P28595, line 3, so that it is not generalized, and highlights that the linear dependency concerns only the measurements: "*The measured viscosity/shape-transition RH has near linear dependency of the temperature*".

9, P28596, line 5-7, SOA from difference precursors may behave differently. It is suggested to rephrase this statement and limited to a-pinene SOA as the manuscript only showed a-pinene SOA data.

We agree with the Reviewer that only alpha-pinene SOA was investigated and the method is not guaranteed to work with other SOA precursors. Therefore we modified the last paragraph in chapter 4.5. We added the word "alpha-pinene" before SOA in the first and in the second sentence and we removed the last sentences in the paragraph and replaced them. The revised paragraph states the following: "*Our method to detect the viscosity/shape-transition of alpha-pinene SOA is likely limited to laboratory experiments with high number concentrations promoting the formation of non-spherical SOA particle aggregates. Though our limited data do not support the hypothesis that SOA particles in the lower troposphere might be non-spherical, we have demonstrated the first* *non-invasive method to study the viscosity of SOA particles formed by ozonolysis of gaseous alpha-pinene. Moreover, the transition timescales that we observed, 10s of minutes, are relevant to those that we can expect in the atmosphere. Therefore, the viscosity/shape-transition RH that we report is relevant for the atmospheric processes. The present study focused on understanding the humidity effect on the viscosity transition temperature of a~single SOA component. The method could also be used in future studies to study SOA shape transitions of other SOA precursors.*"

10, P28597, line 22, "viscosity transition temperature RH at temperatures.." typo?

We removed the additional word "temperature". The corrected sentence is now: *"Generally, our results improve the understanding of the viscosity-transition RH at temperatures above the homogeneous freezing point."*

11, Fig.4, unit of particle concentration is missing.

We thank the Reviewer for noticing the missing units. We added in Figs. 4 and 5 "dN dlogD_p [cm-3]" above the color bar.

12, Fig.8 Caption, two "is" in last sentence.

We removed the additional "is".

Kidd, C., Perraud, V., Wingen, L. M., and Finlayson-Pitts, B. J.: Integrating phase and composition of secondary organic aerosol from the ozonolysis of a-pinene, P. Natl. Acad. Sci. USA, 111, 7552–7557, doi:10.1073/pnas.1322558111, 2014.

Wang, B. B.; O'Brien, R. E.; Kelly, S. T.; Shilling, J. E.; Moffet, R. C.; Gilles, M. K.; Laskin, A. Reactivity of liquid and semisolid secondary organic carbon with chloride and nitrate in atmospheric aerosols. J. Phys. Chem. A 2015, 119, 4498−4508.

Song, M., Liu, P. F., Hanna, S. J., Li, Y. J., Martin, S. T., and Bertram, A. K.: Rel- ative humidity-dependent viscosities of isoprene-derived secondary organic material and atmospheric implications for isoprene-dominant forests, Atmos. Chem. Phys., 15, 5145-5159, doi:10.5194/acp-15-5145-2015, 2015.

We thank the anonymous Reviewer for his/her and encouraging comments. We found that the comments helpful and by answering them we were able to improve the quality of our manuscript. Here, we give detailed answers to the comments. The Reviewer comments are *in italics* **and our reply** in blue standard text**.**

Järvinen et al. introduce a new method of probing the viscosity of SOA as a function of RH and temperature, and they apply this method to determine information related to the viscosity of SOA generated from the oxidation of alpha-pinene. The experiments are novel and extremely important, as they provide laboratory data related to the viscosity of SOA at cold temperatures. Currently this type of information is very limited, yet this type of information is needed to understanding ice nucleation by SOA in the atmosphere. Although the experiments are excellent and the information provided is crucial, I do have comments on the data interpretation that should be addressed before publication. Once these issues are addressed, I highly support publication in ACP.

We thank the Reviewer for this very positive general comment. For the revised version, we have improved the data interpretation based on the Reviewer's suggestions. We are more careful with the term “viscosity-transition” and have renamed it as “viscosity/shape-transition”. We now clearly state already in the Introduction that the method does not directly measure the viscosity of the particles, but their shape. The change in the particle shape can be related to changes in the viscosity. We estimated the viscosity of the particles during their transition and have derived a viscosity of 10^7 Pa s. This value was compared to literature to estimate the physical meaning of our observations. In the revised manuscript we, therefore, omit assuming that the particles were in an aqueous state after the transition. We also do not discuss the results in the context of glass-transition. We hope that the revisions have brought the clarity to the manuscript that the Reviewer was looking for.

Comments on interpretation of experimental results:

1) Page 28596, line 20. Consider replacing “for the phase transition” with “for the aspherical to spherical transition” since the authors have not proven that they have measured a phase transition. For example they haven’t proven that they are measuring the relative humidity for the glass to semisolid phase transition (which occurs around 10^12 Pa s) or the semisolid to liquid transition (which occurs at 100 Pa s).

We agree with the Reviewers suggestion and changed the phase transition to “the transition from aspherical to spherical”.

2) Conclusions, line 4. Would “aspherical to spherical transition” be more appropriate than “viscosity transition”? Viscosity is expected to change (i.e. transition) with RH in a continuous manner for most RH values. For example at warm temperatures and high RH values, as the RH is increased the viscosity is expected to change (i.e. transition) yet the experiments described here are not sensitive to these changes.

The Reviewer is correct, when pointing out that we do not directly measure the viscosity transition, but shape change. This shape change can be related to a viscosity transition, as discussed above. To be correct, we modified the second sentence in the conclusions following: “*Here, we estimated the viscosity of α-pinene SOA at different atmospherically-relevant temperatures and relative humidities using a new optical and non-invasive in-situ method*”. In the following sentence, we explain what the method measures directly: “*We used near-backscattering depolarisation to measure the asphericity of the SOA particles and their shape change to spherical that took place at viscosity of around* 10^7 *Pa s.*”

3) Page 28587 line 1. Consider removing "during a phase transition" since the authors are not necessarily probing a phase transition. Rather they could be just sensitive to when the viscosity falls below a certain value.

We removed "during a phase transition" and just state "during RH increase".

4) Abstract. The authors claim that they are measuring the transition from the amorphous viscous state to a liquid state. However, the experimental observations (non- spherical to spherical transition) may occur at viscosities much higher than a liquid state, which has been defined in the atmospheric literature as a material with a viscosities less than 100 Pa s.

We agree with the reviewer. The added viscosity investigations showed that the alpha-pinene SOA particles had a relatively high viscosity of 10^7 Pa s during their shape-transition. Therefore, we cannot assume that after this transition the particles would have been liquid, i.e. have viscosity less than 100 Pa s. We modified this sentence in the abstract following: "*we deployed a new in-situ optical method to detect the viscous state of α-pinene SOA particles and measured their transition from the amorphous highly viscous state to states of lower viscosity".*

5) Page 28595, line 9, the authors refer to the full deliquescence relative humidity. Please define what they mean by full deliquescence relative humidity. Also, how do they know that the so-called viscosity transition occurs near the full deliquescence relative humidity?

We removed this paragraph discussing the full deliquesce RH. Instead we estimated the viscosity of the alpha-pinene SOA particles and discussed our findings in the view of previous studies.

6) Page 28595, line 11-13. Here the authors are discussing the timescale for water diffusion within the particle bulk. The authors should estimate what this time scale is based on recent published diffusion coefficients for water in SOA and include these estimated time scales in the manuscript. Based on these values is water diffusion the rate limiting step in their experiments? See [Price et al., Chemical Science, 2015; Lienhard et al., ACP, 2015].

We estimated the water diffusion time scales based on the recommended work by Price et al. 2015 and Lienhard et al. 2015. The diffusion rate in our experiments is in the order of seconds, so we can say that the water diffusion rate is not a limiting step.

7) In previous publications the time scale for aspherical particles to transition to spherical particles has been used to estimate viscosities [Zhang, Sanchez et al. ACPD, 2015; Pajunoja et al. Aerosol Sci. Tech. 2014]. Have the authors considered estimating viscosities from their observables? I think the current paper would be clearer if the authors estimated viscosities from their results.

We used the method in Pajunoja et al. (2014) to estimate the viscosity of the SOA particles base on the transition time to spherical. This estimation is showed and discussed in the chapter 4.5. We agree that adding this estimation, we can bring clarity to the revised version and better discuss the physical meaning of the shape transition.

Experimental issues:

1) Page 28586. Line 16-17. The authors state that two thermocouples near the wall were excluded due to wall temperature effects. I assume this means that the temperature close to the wall was colder? The experiments involved adding a flow of humidified gas and mixing the flow in the *chamber with a fan. Is it possible that the temperature and relative humidity was different close to the walls, and the aspherical to spherical transition occurred close to the walls, not in the middle of the chamber? If this was the case, the temperature and RH reported may be different than the temperature and RH at which the aspherical to spherical transition occurred?*

Excluding the two thermocouples closest to the wall is necessary in cloud expansion experiments, when we cool the chamber volume but the chamber walls stay at a constant temperature. This creates a temperature gradient that could bias the measurements. However, in the experiments presented in this paper such expansion experiments were not conducted, so excluding the two thermocouples next to the wall is not necessary. We checked the differences between the thermocouples and came into a conclusion that they agree quite well with each other. The maximum temperature difference they showed was 0.2 K. This difference is the same order as the measurement uncertainty of the thermocouples. Therefore, we don't think that significant temperature gradients existed during the experiments that could have led to biases. We removed the phrase “ *excluded due to wall temperature effects”* so that the reader is not mislead.

Comparison with Koop et al. 2011:

1) Page 28595, Line 20-25: I do not understand the argument that the measured “viscosity transition” can be compared to the relative humidity of the glass transition (RHg) in atmospheric context. The glass transition occurs at a viscosity of roughly 10ˆ12 Pa s. To argue that the “viscosity transition is comparable to the glass transition, I think one would need to argue that both transitions occur at roughly the same viscosity? Can the authors estimate that viscosity at which their aspherical to spherical phase transition occurred?

We estimated the viscosity during the transition, and indeed the shape transition occurs at lower viscosities. Therefore, we removed this statement.

2) Page 28595, line 27-29. “Our results suggest the relationship between the transition C11151

RH and the temperature is more linear than predicted by Koop et al. 2011. This may be especially relevant at high RH, where we can expect that the transition might take place at a much higher temperature than predicted by Koop”. I suggest the authors should modify this text since all the experimental results shown here are within the estimates presented by Koop et al. 2011 (green shaded region in Figure 11).

We modified the sentence the following: “*Moreover, our results suggest the relationship between the transition RH and the temperature is more linear than predicted by Koop et al. (2011), although measurements at colder temperatures are missing. To understand the viscosity transition of alpha-pinene SOA particles at high RH in the cirrus regime, measurements at colder temperatures are recommended.*”. We also removed the sentence: “*where other studies might suggest that it relax*” from atmospheric implications.

Minor points:

2) Page 28581. Line 4. Should “isotropic” be deleted?

We agree that the word “isotropic” is not necessary here and, thus, we removed it.

3) Page 28587, line 15. “the SOA particles were generated and grown in the chamber by continuous oxidation of alpha-pinene with ozone”. Should this be “. . . by continuous oxidation of alpha-pinene with ozone and OH radicals”?

We did not limit the formation of OH radicals, so the Reviewer's suggestion is correct. We modified the sentence accordingly.

4) Figure 5. In the figure caption it is stated that the linear depolarisation ratio stayed below the detection threshold during the entire experiment. However, at times between 6:00 and 7:00 it looks like the linear depolarisation reaches as high as 0.1. This seems to be well above the LOD. Please discuss.

The signal between 6:00 and 7:00 is purely noise as the particles were too small to scatter enough light to the detectors. Only after 7:00 we had enough signal to reliably determine the depolarisation ratio. However, the Reviewer is correct, when pointing out that we do not mention the noise in the text. In the revised version we added a sentence to the figure caption: "*At the beginning of the growth (6:00-7:00) the SOA particles were too small to efficiently scatter light and the signal shown in panel (c) at that time is mostly noise. After the particles were larger than 100 nm, the linear depolarisation ratio stayed below the detection threshold.*" We also modified the figure 4, by adding the unfiltered depolarisation data, since the depolarisation data shown in that figure was filtered from noise. Now we are more consistent, as background noise is always present if particle concentrations are low.

5) Was figure 8 discussed in the main text? If not, should it be removed from the manuscript?

The figure 8 was discussed in the third paragraph in the chapter 4.3. The purpose for this figure was to show that circular depolarisation ratio is always higher than linear, i.e. it could be potentially more sensitive to particle shape.

Manuscript prepared for Atmos. Chem. Phys. Discuss.
with version 2014/09/16 7.15 Copernicus papers of the LaTeX class copernicus.cls.
Date: 8 March 2016

Observation of viscosity transition in α-pinene secondary organic aerosol

E. Järvinen[1], K. Ignatius[2], L. Nichman[3], T. B. Kristensen[2], C. Fuchs[4], C. R. Hoyle[4,8], N. Höppel[1], J. C. Corbin[4], J. Craven[5], J. Duplissy[6], S. Ehrhart[7], I. El Haddad[4], C. Frege[4], S. J. Gates[4], H. Gordon[7], T. Jokinen[6], P. Kallinger[9], J. Kirkby[7,10], A. Kiselev[1], K.-H. Naumann[1], T. Petäjä[6], T. Pinterich[9], A. S. H. Prevot[4], H. Saathoff[1], T. Schiebel[1], K. Sengupta[11], M. Simon[10], J. Tröstl[4], A. Virtanen[12], P. Vochezer[1], S. Vogt[1], A. C. Wagner[10], R. Wagner[1], C. Williamson[10,13,14], P. M. Winkler[9], C. Yan[6], U. Baltensperger[4], N. M. Donahue[15], R. C. Flagan[16], M. Gallagher[3], A. Hansel[17], M. Kulmala[6], F. Stratmann[2], D. R. Worsnop[18], O. Möhler[1], T. Leisner[1], and M. Schnaiter[1]

[1]Karlsruhe Institute of Technology, Institute for Meteorology and Climate Research, P.O. Box 3640, 76021 Karlsruhe, Germany
[2]Institute for Tropospheric Research (TROPOS), 04318 Leipzig, Germany
[3]School of Earth, Atmospheric and Environmental Sciences, University of Manchester, Manchester, M13 9PL, UK
[4]Laboratory of Atmospheric Chemistry, Paul Scherrer Institute, Villigen, Switzerland
[5]California institute of technology, department of chemical engineering, Pasadena, CA, 91125, USA
[6]Helsinki Institute of Physics and University of Helsinki, Department of Physics, Helsinki, Finland
[7]CERN, 1211, Geneva, Switzerland
[8]Swiss Federal Institute for Forest Snow and Landscape Research (WSL)-Institute for Snow and Avalanche Research (SLF), 7270 Davos, Switzerland

[9]Faculty of Physics, University of Vienna, Austria
[10]Institute for Atmospheric and Environmental Sciences, Goethe-University Frankfurt am Main, Campus Riedberg Altenhöferallee 1, 60438 Frankfurt am Main, Germany
[11]University of Leeds, School of Earth and Environment, LS2-9JT Leeds, UK
[12]Department of Applied Physics, University of Eastern Finland, Kuopio, Finland
[13]NOAA Earth Systems Research Laboratory (ESRL), Chemical Sciences Division, 325 Broadway, Boulder, Colorado 80305, USA
[14]Cooperative Institute for Research in Environmental Sciences (CIRES), University of Colorado Boulder, UCB 216, Boulder, Colorado 80309, USA
[15]Center for Atmospheric Particle Studies, Carnegie Mellon University, 5000 Forbes Ave., Pittsburgh PA 15213, USA
[16]California Institute of Technology, Division of Chemistry and Chemical Engineering, Pasadena, California 91125, USA
[17]Institute for Ion and Applied Physics, 6020 Innsbruck and Ionicon Analytik GmbH, 6020 Innsbruck, Austria
[18]Aerodyne Research, Inc., Billerica, MA 08121, USA

Correspondence to: E. Järvinen (emma.jaervinen@kit.edu)

Abstract

Under certain conditions, secondary organic aerosol (SOA) particles can exist in the atmosphere in an amorphous solid or semi-solid state. To determine their relevance to processes such as ice nucleation or chemistry occurring within particles requires knowledge of the temperature and relative humidity (RH) range for SOA to exist in these states. In the CLOUD (Cosmics Leaving Outdoor Droplets) experiment at CERN (The European Organisation for Nuclear Research), we deployed a new in-situ optical method to detect the ~~viscosity~~ viscous state of α-pinene SOA particles and measured their transition from the amorphous ~~viscous to liquid state~~ highly viscous state to states of lower viscosity. The method is based on the depolarising properties of laboratory-produced non-spherical SOA particles and their transformation to non-depolarising spherical ~~liquid particles during deliquescence~~ particles at relative humidities near the deliquescence point. We found that particles formed and grown in the chamber developed an asymmetric shape through coagulation. A transition to spherical shape was observed as the RH was increased to between 35~~% at -10°~~ % at -10 °C and 80~~% at -38°~~ % at -38 °C, confirming previous calculations of the viscosity transition conditions. Consequently, α-pinene SOA particles exist in a viscous state over a wide range of ambient conditions, including the cirrus region of the free troposphere. This has implications for the physical, chemical and ice-nucleation properties of SOA and SOA-coated particles in the atmosphere.

1 Introduction

Organic particulate material is abundant in Earth's atmosphere. Biogenic and anthropogenic sources emit volatile organic compounds (VOCs), which are oxidised through a cascade of chemical reactions into extremely low volatility vapours that condense into the particle phase to form secondary organic aerosol (SOA) (Hallquist et al., 2009). Biogenic VOCs are much more abundant than anthropogenic VOCs (Guenther et al., 1995; Jimenez et al., 2009) and monoterpenes such as α-pinene are found throughout the continental boundary layer, particularly in boreal forest regions (e.g., Tunved et al., 2006; Laaksonen et al., 2008). After formation, SOA influences climate on a global scale directly by scattering and absorbing solar radiation and indirectly through aerosol-cloud interactions. Locally, SOA can affect air quality and human health (e.g., Nel, 2005; Huang et al., 2014). However, the chemical and physical processes that determine the properties of SOA particles are complex, and our understanding of these processes is limited (Hallquist et al., 2009; Hoyle et al., 2011).

Recently, considerable attention has been given to water uptake and viscous properties of SOA. It has been found that SOA particles can exist in the atmosphere in an amorphous semi-solid or solid state (Virtanen et al., 2010; Koop et al., 2011; Renbaum-Wolff et al., 2013; Pajunoja et al., 2014). The existence of these states has several atmospheric implications. Molecular diffusion in the condensed phase affects the gas uptake by viscous SOA particles and can, therefore, alter the SOA particle lifetime in the atmosphere (Shiraiwa et al., 2011). In addition, water uptake is inhibited in the viscous particles (Riipinen et al., 2012), limiting the SOA growth under conditions in which SOA would typically grow hygroscopically (Swietlicki et al., 2008; Pajunoja et al., 2015). This, in turn, influences the aerosol direct effect on radiative forcing. More recent studies have shown that the viscous SOA particles or their proxies can act as ice nuclei (IN) (Murray et al., 2010; Wagner et al., 2012; Wang et al., 2012; Wilson et al., 2012; Schill et al., 2014), thus influencing cloud cover, cloud optical properties, and precipitation.

In order to understand the climatological influence of the viscous state of SOA particles, detailed knowledge of the temperature and relative humidity (RH) ranges in which SOA can persist in a solid or semi-solid state is needed. Several experimental methods have been developed to measure the transition temperature or RH between different SOA phase states. A direct way to measure the glass transition temperature, ~~T_g~~T_{g}, of SOA substances is to use differential scanning calorimetry ~~(DSC, Zobrist et al. (2008))~~(DSC, Zobrist et al., 2008) . However, this method requires the removal of the semivolatile aerosol particles from the surrounding gas, which can change the state, shape, or composition of the SOA particles (Zhang et al., 2015) . In contrast, indirect methods allow the sampling of the SOA particles with their surrounding gas. As indirect methods, they do not directly measure ~~T_g~~T_{g}, but rather probe the change in the SOA particle mechanical or aerodynamical properties with temperature or RH. These methods include the bounce method that exploits the fact that solid or semisolid particles rebound in an impactor plate, whereas liquid particles adhere. A low pressure impactor ~~(ELPI; Virtanen et al. (2010); Saukko et al. (2012))~~ (ELPI; Virtanen et al., 2010; Saukko et al., 2012) has been used for this purpose and, recently, the method is extended to work at atmospheric pressures (Bateman et al., 2014). Moreover, the so-called *poke-flow* method (Renbaum-Wolff et al., 2013) and the shatter technique (Schill et al., 2014) use mechanical forces to disturb single particles and the response to the mechanical stress can be linked with a phase state. Finally, the particle phase state can be determined with measurement of their aerodynamic shape factor (Zhang et al., 2015).

Although these methods provide useful insights into the nature of the SOA particles, the SOA aerosol has been sampled and passed through an instrument, in which their environment is altered. This may result in a change in the material properties. In an effort to minimise biases due to these perturbations, we have employed a new optical method that provides a noninvasive probe of shape or structural anisotropy that may be present in solid or highly viscous semisolid SOA particles (Virtanen et al., 2010; Adler et al., 2013; Pajunoja et al., 2014; Schill et al., 2014; Zhang et al., 2015), but that is quickly erased in low viscosity droplets as they relax toward the most energetically favourable state, i.e., spherical droplets that are homogeneous throughout their volumes.

For a perfectly isotropic, spherical particle, light that is scattered directly back toward its source, i.e., in a direction of 180~~°~~° from that of the incident light, retains its initial polarisation state. Whether it results from deviations from spherical symmetry, or from structural inhomogeneities, anisotropy in the optical properties leads to depolarisation. A measurement of the extent of depolarisation in the backscattered light probes the magnitude of the anisotropy and, hence, the ability of the particle to relax to its low-energy state. This signal thus reflects the viscosity of the material that comprises the particle, provided that some mechanism has previously introduced anisotropy.

Here, we present a new approach based on in situ measurement of depolarisation, and use it to study the effect of temperature and ~~relative humidity~~ RH on the viscosity transitions that SOA particles may undergo as they become solvated with water at high humidity. This paper is organised as follows. The new method depends on how different types of anisotropy affect depolarisation of light scatted by the small (sub-micron) SOA particles that are found in the atmosphere. We begin, therefore, with theoretical and modelling studies of the effects of size, shape, and internal structure on the depolarisation signals that we may expect. The modelling studies allow us to constrain the range of particle sizes and concentrations for which the method is useful, and proved central to the design and optimisation of an instrument capable of measuring the viscous transition under atmospheric conditions. Moreover, they aid in understanding the relative importance of shape and structural anisotropy in the measurements.

We then describe the experimental method, the instrument that has been developed, and instrument characterisation experiments that assess the limits to the sensitivity of the depolarisation measurements. We ~~have measured the~~ define an instrumental-based viscosity~~transition of a~~/shape-transition RH that describes the RH value, where the particles were observed to be spherical or isotropic according to our method. The viscosity/shape-transitions are measured for a model SOA system, i.e., the SOA produced by oxidation of ~~$\alpha-$pinene~~α-pinene. The experiments were conducted in the CERN CLOUD chamber, an environmental chamber that has unique capabilities to simulate conditions throughout the troposphere while maintaining the cleanliness required for new particle formation studies (Schnitzhofer et al., 2014). We describe the experimental facility, key measurement methods that were employed, and experimental procedures.

Experimental results are described, beginning with those from the instrument characterisation studies, but then focusing on the dynamics of the SOA particles, the evolution of their properties, and the viscosity~~transition of the $\alpha-$pinene~~ /shape-transition of the α-pinene SOA. We continue the paper by a discussion of the atmospheric implications of our findings, and finish with conclusions.

2 Theoretical ~~Considerations~~considerations

The depolarisation ratio is a measure of how strongly the polarisation state of incident light is altered during scattering by particles. Isotropic spherical particles do not induce linear or circular depolarisation in the exact backward direction, whereas non-spherical particles alter the depolarisation state of incident light depending on their size, shape, and refractive index. Therefore, depolarisation measurements can be used to determine the ~~asphericity of isotropic particles~~particle asphericity. The magnitude of the depolarisation ratio can, in the case of aerosol particles, vary from only few per cent (in the case of sea salt) to up to 0.4 (in the case of dust aerosol) (Sakai et al., 2010). Solid or semi-solid amorphous particles may also induce depolarisation due to internal structures or inhomogeneous refractive index. In this case the depolarisation will depend on the gradient and/or variation of the refractive index as well as the size of the particle. In the case of sub-micron particles, the scale of the variation in particle properties is restricted by the size, and hence we can expect a maximum depolarisation ratio of 0.01 due to particle inhomogenities, whereas the probable depolarisation ratios are well below that (Li et al., 2005; Dlugach and Mishchenko, 2015).

To quantify the extent of depolarisation, we define the the depolarisation ratio, ~~$\delta_{L,C}$ (indices L,C~~ $\delta_{\mathrm{L,C}}$ (indices L, C denoting the liner or circular incident depolarisation state) as the ratio of the intensity of the parallel polarised light, $I_{\parallel}$, to the perpendicular polarised light, $I_{\perp}$, in the backscatter direction when the particle is illuminated with perpendicularly polarised light. For a perfect measurement, we could take the ratio directly. In any real measurement there will be some background contribution to these two signals in the form of molecular scattering and scattering from chamber walls. Therefore, we subtract the background intensities ~~$I_{\parallel}^{bg}$ and $I_{\perp}^{bg}$~~ $I_{\parallel}^{\mathrm{bg}}$ and $I_{\perp}^{\mathrm{bg}}$ measured in the absence of scattering particles from the measured scattered light intensities during particle measurements, defining ~~$\delta_{L,C}$~~

~~as~~ $\delta_{\mathrm{L,C}}$ as

$$\delta_{\mathrm{L,C}} = \frac{I_{\parallel} - I_{\parallel}^{\mathrm{bg}}}{I_{\perp} - I_{\perp}^{\mathrm{bg}}}. \tag{1}$$

$$\delta_{L,C} = \frac{I_{\parallel} - I_{\parallel}^{bg}}{I_{\perp} - I_{\perp}^{bg}},$$

We modelled the depolarisation ratio to assess the sensitivity of this method to the small particles that are produced in the environmental chamber and that will be used for studies of the viscosity transition. We ignore the effect of anisotropy and consider only the influence of the particle asphericity on the depolarisation ratio. This can be estimated using a T-matrix approach in a regime that is appropriate for particles whose size is of the order of the wavelength of the incident light (Mishchenko et al., 1996). We performed T-matrix computations using the aforementioned constraints to model the expected depolarisation properties of growing SOA particles in our experiments. The simulations were done for a particle size distributions with geometric mean diameters (GMD) ranging from 100 to 1400~~nm~~ nm and with a narrow geometric standard deviation (GSD) of 1.1, as would be expected when the primary growth mechanism is condensation. The refractive index ~~was chosen to be 1.5+0i after Schnaiter et al. (2005) , with the assumption that~~ of α-pinene SOA at near room temperatures has been shown to vary between 1.4 and 1.6 (Schnaiter et al., 2005; Kim et al., 2010; Redmond and Thompson, 2011) . As we do not have the information on the refractive index of viscous α-pinene SOA ~~does not differ significantly from that of an aqueous solution of α-pinene SOA~~particles, we assumed in the modelling study a refractive index of 1.5+0i after Schnaiter et al. (2005) . Further details on the computational procedures used to model particle depolarisation ratios can be found in Schnaiter et al. (2012).

2.1 Simulation results

The SOA particles were modelled with prolate spheroids. Prolate spheroids have a greater polar radius than equatorial radius, having the form of a symmetrical egg. In the T-matrix formalism the aspect ratio of these particles describes the relationship of the equatorial radius to the polar radius and is therefore always smaller than 1 (Fig. 1). Since the aspect ratio of the SOA particles is unknown, we performed the calculations with aspect ratios ranging from 0.91 to 0.5 (Fig. 2), where the largest aspect ratio of 0.91 represents the smallest deviation from a spherical shape and the smallest aspect ratio of 0.5 the largest deviation. Figure 2 shows that both the linear and circular depolarisation ratios increase with increasing GMD of the particles. The increase in the depolarisation ratio is significant up to 800 nm, whereafter the influence of the size of the particles decreases. Moreover, the higher the aspect ratio (the closer the particles are to being spherical), the lower is the expected depolarisation ratio. In the least aspherical case (aspect ratio 0.91), we estimate that the SOA particles have close to zero depolarisation ratios at GMD below 400~~nm and a~~ nm and a maximum depolarisation ratio that is close to 0.1 (linear depolarisation) or to 0.25 (circular depolarisation) at GMD of 1400~~nm~~ nm.

As a result of these modelling studies, we can estimate that the internal inhomogeneity of SOA particles will most likely have only small, almost negligible effect on the depolarisation ratio and that the depolarisation ratio is mainly determined by the degree of particle asphericity. The T-matrix results showed that the particles with a GMD from 50 to 800 nm will only produce extremely small depolarisation ratios, which will be challenging for the depolarisation measurements. A high degree of sensitivity is required for the depolarisation instrument, otherwise, the particles would require growth to sizes larger than 1 µm.

3 Experimental ~~Methods~~methods

3.1 Depolarisation measurements

We developed a new in-situ depolarisation instrument, SIMONE-Junior, with the necessary sensitivity to detect very low depolarisation ratios. SIMONE-Junior is based on the design of the first SIMONE instrument (Schnaiter et al., 2012), which is installed at the cloud chamber facility AIDA of the Karlsruhe Institute of Technology, with few improvements that have been implemented to attain the sensitivity and stability requirements that were identified in the simulations. SIMONE-Junior uses a continuous wave (cw) laser (Coherent 552~~nm~~ nm OBIS laser, 20~~mW~~ mW) to create a polarised and collimated light beam that is directed horizontally across the chamber (Fig. 3). The incident linear polarisation state of the laser beam can be aligned either parallel or perpendicular to the scattering plane by a liquid crystal polarisation rotator. Moreover, in contrast to the AIDA SIMONE, a liquid crystal variable retarder, ~~cabable~~ able to be operated as a quarter-wave plate, was introduced to the system to allow generation of circularly polarised light. The orientation of the circular depolarisation can be changed from right-handed to left-handed, although in this study we used only right-handed circular incident polarisation.

Two telescopes collect the laser light scattered from the centre of the aerosol chamber at an angle of 4~~°~~ ° in the forward direction and 176~~°~~ ° in the backward direction. While the intensity in the forward scattering angle is directly measured with a photonmultiplier tube, the intensity in the backward scattering angle is decomposed into its polarisation components by a Wollaston prism. In the case of circular polarisation, the scattered light is first retarded to linear polarisation with a second liquid crystal variable retarder before the Wollaston prism.

3.2 Experimental setup

The experiments presented here were conducted at the CERN CLOUD chamber ~~(Kirkby et al., 2011; Duplissy et al., 2015)~~ (Kirkby et al., 2011; Duplissy et al., 2015; Hoyle et al., the CLOUD8 (~~November-December~~ November–December 2013) and CLOUD9 campaigns (~~September-November~~ September–November 2014). The chamber consists of a 26 m^3 stainless steel cylinder that is located inside a~~housing with thermal insulation~~ thermally insulated housing. The temperature of the chamber can be varied from ~~-60°C~~ −60 to 100~~°C and it~~ °C and is controlled by regulating the temperature of air flowing around the chamber and inside the thermal housing. During the CLOUD8 and CLOUD9 campaigns, the temperature inside the chamber was measured with a string of six thermocouples positioned horizontally at different distances between the wall and the chamber centre. We used the mean of the ~~four inner~~ thermocouples as a representative measure of the temperature in the chamber volume.

In the course of the experiments, air from the chamber was constantly sampled; and this sampled air was replaced with humidified artificial air to maintain a constant pressure inside the chamber. The artificial air was created by evaporating liquid nitrogen and oxygen, and humidified by passing part of the flow through a Nafion humidifier to achieve a chosen constant relative humidity (RH). Alternatively, the air was passed through a heated line to the chamber, allowing the dew point of the incoming air to be higher than that in the chamber. The heated line was used at temperatures of ~~-30°~~ −30 °C or lower, to enable rapid RH increase. The water vapour was mixed with the main air stream before entering the chamber, which allowed a homogeneous RH throughout the chamber volume after a mixing time of few minutes (Voigtländer et al., 2012). The RH inside the chamber was measured with a chilled mirror dew point hygrometer (MBW, model 973). During CLOUD9 a tuneable diode laser (TDL system) was used to measure water vapour, in addition to the MBW. The newly installed tuneable diode laser system will be described in more detail in the following section.

SOA particles were produced within the CLOUD chamber by ozonolysis of gaseous α-pinene; the two reactant gases were separately fed into the chamber through mass flow controllers. The ozone was monitored with a trace gas monitor (~~O_3~~ O_3 analyser, Thermo Environmental Instruments, Inc., Model 49C); α-pinene was measured by a~~PTR-TOF (~~ Proton Transfer Reaction Time of Flight Mass Spectrometer (PTR-TOF, Ionicon Analytic). The ozone concentration was continuously measured, but, due to high concentrations of α-pinene (over 600~~ppbv~~ ppbv), the PTR-TOF signal saturated, so it could not be measure continuously. The production of SOA was enhanced by ~~UV~~ ultraviolet (UV) photolysis of ozone to form OH radicals. A 50~~W~~ W UV source (Philips TUV ~~130W~~ 130 W XPT lamp) was installed in a quartz tube inserted into the chamber. The formed OH oxidised α-pinene to produce ~~secondary~~ lower volatility organic vapours that nucleated and grew the aerosol particles.

Supporting measurements were provided by a range of instruments that were used to measure the physical and chemical composition of the aerosol particles inside the chamber. The chemical composition of the sub-micron aerosol particles was measured with an Aerodyne high-resolution time-of-flight aerosol mass spectrometer (HR-ToF AMS). From these measurements the atomic oxygen to carbon ratio (O~~/~~ / C) was determined. The size distribution of the aerosol particles was measured with an Ultra-High Sensitivity Aerosol Spectrometer (UHSAS, DMT), which measures the optical sphere equivalent diameter of the particles in a size range from approximately 60 to 1000~~nm and with an SMPS~~ nm and with a Scattering Mobility Particle Sizer (SMPS), which measures the mobility diameter between 30 ~~nm~~ and 500~~nm~~ nm. The total concentration of aerosol particles was measured with a~~CPC (~~ Condensation Particle Counter (CPC, TSI 3010) with a 10~~nm~~ nm cutoff and with a maximum detectable particle concentration of 10 000 cm^{-3} without coincidence corrections.

3.2.1 Relative humidity measurements

During the CLOUD9 campaign a tuneable diode laser (TDL) hygrometer, comparable to the APicT (AIDA PCI in-cloud TDL) instrument as described by Fahey et al. (2014), was used to measure the water vapour content in-situ. The TDL has 1~~Hz~~ Hz time resolution and employs a single optical path of 314~~cm~~ cm once across the mid-plane of the CERN CLOUD chamber. Its main component is a temperature-controlled, 10~~mW~~ mW distributed feedback diode laser (NTT Electronics) at a wavelength of (~~1370±1)~~1370 ± 1) nm. The water absorption line was fitted on-line to determine water concentrations based on well-known spectroscopic constants. The windows mounted on the chamber limited the measurement range to between ~~30 - 1300 Pa~~ 30–1300 Pa water vapour pressure (~~300-13000 ppm~~ 300–13 000 ppm mixing ratio); the measurement uncertainty was ±7~~%~~ % above 100~~Pa~~ Pa and ±10~~%~~ % between 30 and 100~~Pa~~ Pa. The relative humidity in the CLOUD chamber was calculated using these humidity data together with the average temperatures measured with a horizontal string of four calibrated thermocouples at the mid-plane of the chamber. The ~~two thermocouples near the wall were excluded due to wall temperature effect. The~~ TDL hygrometer data enabled determination of the relative humidity even in the presence of clouds in the chamber, with an uncertainty of ±10~~%~~ % above 100~~Pa~~ Pa and ±13~~%~~ % between 30 and 100~~Pa~~ Pa water vapour pressure. The total humidity in the CLOUD chamber was also derived from the measurements from dew point hygrometer (model MBW973, MBW calibration Ltd.) attached to a heated sampling line.

3.2.2 Experimental procedure

The aim of the experiments was to determine if a slightly aspherical particle shape or internal inhomogeneity of the viscous amorphous SOA could be detected by sensitive, near-backscatter depolarisation measurements and, if so, to observe the transition from irregular to a spherical shape during ~~a phase transition as the RH was increased~~RH change. The range of experiments required was determined using the T-matrix modelling together with the lowest detection limit of the SIMONE-Junior instrument as guidelines. ~~Fig.~~ Figure 2 demonstrates that, in order to measure a significant depolarisation signal with the highest aspect ratio (0.91), particles with a GMD of at least 600~~nm~~ nm must be generated. Furthermore, in contrast to atmospheric lidar applications (e.g., Sassen, 1991; Hirsikko et al., 2014), the detection volume of the SIMONE instrument is small, only few ~~cubiccentimeters~~cubic centimetres. This means that we would need a high concentration to have enough particles inside this small detection volume to produce measurable signals. We estimated that an initial concentration of 10 000 cm^{-3} newly formed SOA particles would produce adequate signals once the particles reached the size of 600~~nm~~ nm.

Each experiment commenced with clean, aerosol-free air (background concentration well below 1 cm^{-3} and low RH (ranging from ~~5-15%~~5–15 %). The chamber was kept at 5 mbar overpressure to avoid under-pressure in the sampling instruments. The SOA particles were generated and grown in the chamber by continuous oxidation of α-pinene (maximum concentration ~~∼600 ppbv~~∼ 600 ppbv) with ozone (maximum concentration ~~∼700 ppbv)~~ ∼ 700 ppbv) and OH radicals to form low volatility oxidised organic compounds. SOA nucleation was initiated by injecting α-pinene (10~~ml/min~~ mL min^{-1}) and ozone (1000~~ml/min~~ mL min^{-1}) into the chamber simultaneously for 1 to 7~~minutes~~ min, depending on the chamber temperature, and then turning on the UV light. After 1~~minute~~ min the α-pinene flow was turned off until the freshly nucleated particles had grown to a mean diameter of approximately 100~~nm~~ nm. This produced a near-monodisperse particle population. At this point the α-pinene flow was turned back on and continuously injected into the chamber in order to grow the existing particles without inducing further new particle formation. The initial particle burst typically comprised around 50~~000~~ 000–100 000 cm^{-3} α-pinene SOA particles, which rapidly grew to about 20~~nm~~ nm diameter. After the particles had grown to diameters of approximately 600~~nm~~ nm, losses due to dilution, coagulation and the chamber walls had reduced the particle number concentration to ~~5 000~~ 5000–10 000 cm^{-3}. After a significant depolarisation signal had been detected, we increased the RH in the chamber to search for a transition to the liquid phase. The RH was gradually increased by injecting humidified air (RH 100~~%~~ %) air into the chamber while simultaneously mixing the air inside the chamber with fans. This was continued until the depolarisation signal had decreased to a constant zero-level. These experiments were performed at four different temperatures: ~~-10°C, -20°C, -30°C and -38°~~ −10, −20, −30 and −38 °C.

In addition to these transition experiments, we performed one reference run with a higher starting RH (~~60-70%) at -20°~~60–70 %) at −20 °C. The nucleation and growth of the α-pinene SOA particles was conducted in the same way as the other experiments but the high RH was kept constant throughout. The purpose of this reference run was to produce a similar size distribution of α-pinene SOA particles as in the viscosity-transition runs, while ensuring that the state of the particles did not change, i.e., remained liquid, so they could not induce depolarisation. This run was used to verify the depolarisation method for a SOA system and to exclude the possibility of artifacts. The operating conditions for the reference run and all the viscosity-transition runs are listed in Table 1.

4 Results and ~~Discussion~~discussion

4.1 Sensitivity of the depolarisation measurements

Imperfect alignment and non-ideal behaviour of the optical components can induce crosstalk between the parallel and perpendicular channels in the backward scattering direction, i.e., in the perpendicular channel a percentage of the parallel intensity is measured and vice versa. This crosstalk ultimately determines the limit of detection (LOD) for the depolarisation ratio. The LOD can also be defined as the depolarisation crosstalk that is measured in the case of spherical particles.

To determine the LOD, we measured the depolarisation ratio of laboratory-generated sulphuric acid (SA) solution droplets. SA droplets are known to be spherical (e.g., Schnaiter et al., 2012), and since in the calibration we restrict to sub-micrometer sizes, the SA particles should not introduce linear or circular depolarisation at the measurement angle of SIMONE-Junior. Nevertheless, we measured a finite depolarisation in the calibration experiments; this signal represents the crosstalk from the parallel channel to the perpendicular channel. To minimise this depolarisation crosstalk, we optimised the alignment of the optical components by separately rotating the optical planes of each component until a minimum depolarisation signal was measured. The minimum crosstalk depolarisation signal in the case of linear (parallel) incident polarisation was 0.002, and, in the case of circular (right-handed) incident polarisation, 0.015. Moreover, it has to be kept in mind that the alignment of the instrument may change over time, as the instrument is mounted on a~~chamber (section~~ chamber (Sect. 3.2, Fig. 3), whose walls move during the 200~~mbar~~ mbar pressure expansions used for other experiments (a maximum displacement of 0.5~~°~~ ° was observed), and may not return to the exact original position. This also means that the LOD will increase from the calibration value. To be absolutely confident that a measured depolarisation signal is significant, we specified the LOD for linear depolarisation to be 0.01 and for circular depolarisation to be 0.02. If the depolarisation ratio is below these thresholds, we consider the particles indistinguishable from spherical according to our method.

4.2 Growth and coagulation of the α-pinene SOA particles

We performed eight SOA nucleation and growth experiments in the CLOUD chamber using identical initial conditions described in ~~section~~ Sect. 3.2.2. Each experiment resulted in a nucleation event that was followed by rapid growth of the α-pinene SOA particles, producing a narrow particle size mode. Two examples of the growth of a single narrow mode are shown in Figs. 4 and 5. We fitted a log-normal distribution to the particle size distribution data to retrieve GMD and GSD. The ~~mean modal diameters~~ GMD are shown in the first panels, and the GSD together with number concentration in the second panels. From the log-normal fit results, we see that the two runs presented in Figs. 4 and 5 are almost identical with respect to the particle size distribution, even though they were conducted at different temperature and humidity conditions. Both size distributions are narrow with GSD variations between 1.05~~-1.2~~–1.2, and show similar total number concentrations. In each case, particles ~~grow~~ grew beyond 700~~nm~~ nm. The similarities between these two runs is important for interpreting the depolarisation signals, as will be shown later.

Continuous addition of trace gases during RUN1_-20C, RUN_-30C and RUN_-38C led to undesired nucleation events leading to a bimodal distribution of large (main mode with highest concentration) and small particles (secondary nucleation). The additional nucleation event always occurred before the viscosity-transition RH was reached, so we can assume that the state of the newly formed α-pinene SOA particles was highly viscous. This assumption will be verified later with the depolarisation data.

The high SOA particle concentration led to the formation of aggregates by coagulation inside the chamber. The coagulation process becomes an important determinant for the shape of the particles at sizes larger than 30~~nm~~ nm; it has been suggested that sub-30~~nm~~ nm SOA particles are sufficiently liquid (Virtanen et al., 2011) that they coalescence upon coagulation and, therefore, remain spherical. We estimated the coagulation rate using the COSIMA model of Naumann (2003), which was initialised with the size distribution measurements from the SPMS and with an estimated particle density of 1.25~~$g\ cm^{-3}$~~ $\mathrm{g\,cm^{-3}}$. The sticking probability was set to 1 in the model. Figure 6 shows the calculated coagulation rate together with the total concentration from SMPS for the experiment RUN2_-10C (Fig. 4). A maximum concentration of 100 000~~cm^{-3}~~ $\mathrm{cm^{-3}}$ was reached, which led to a coagulation rate of 10~~$cm^{-3}s^{-1}$~~ $\mathrm{cm^{-3}\,s^{-1}}$. At 17:30 UTC the time integral of the coagulation rate was 23 000~~cm^{-3}~~ $\mathrm{cm^{-3}}$, which gives an estimate of the number of particles involved in the coagulation process. This number is of the same order as the total number concentration (25 000~~cm^{-3}~~ $\mathrm{cm^{-3}}$) measured at the same time, indicating that the majority of the SOA particles were involved in coagulation processes and can be expected to have formed aggregates. As the particle number concentration decreases, the aggregation rate decreases to well below 1~~$cm^{-3}s^{-1}$~~ $\mathrm{cm^{-3}\,s^{-1}}$, making coagulation unimportant in the later phase. We can therefore expect that the SOA particles become aspherical aggregates at the beginning of the run and these aggregates subsequently ~~grew~~ grow by condensation, forming quasi-spheroidal particles (Fig. 7), if the growth takes place when the particles are in a viscous phase.

The nucleation and growth conditions for the SOA particles in these experiments at the CLOUD chamber are unlikely to be fully representative of the conditions where SOA is formed in the atmosphere ~~(e.g., Dal Maso et al., 2005; Kulmala et al., 2007; Kirkby et al., 2011; Kulmala et al., 2013; Riccob~~ Viscous biogenic SOA particles have been observed to form in nucleation events in the boreal forest (Virtanen et al., 2010), where the concentrations of particles larger than 25~~nm~~ nm are typically below 100 000~~cm^{-3}~~ $\mathrm{cm^{-3}}$ (Dal Maso et al., 2005). Lower natural particle concentration may not promote the formation of aggregates, and therefore, it is uncertain if natural SOA particles can be expected to be aspherical.

4.3 Depolarisation properties of the α-pinene SOA particles

We conducted a set of experiments with two different initial conditions. The primary experiments were started at low RH, so that the nucleated SOA particles grew in an amorphous solid or semi-solid state. In contrast to these runs, one reference run was made at ~~−20°~~ −20 °C with a high initial RH (~~60-70%~~60–70 %), so that the SOA particles started out in the aqueous phase state. The purpose of this reference run was to validate the depolarisation method on a SOA system that would produce optically isotropic particles, and to exclude possible window artefacts. The SIMONE-Junior instrument is isolated from the chamber with two coated windows that do not change the depolarisation ratio itself, but if material condenses to form a film on the windows, this might affect the measurements.

Figures 4 and 5 show the measured depolarisation ratios of the α-pinene SOA particles during the reference run and during RUN2_-10C. During all the low RH experimental runs below 0~~°~~ °C, a depolarisation ratio above LOD was measured, whereas during the reference run, the depolarisation signal stayed below the depolarisation threshold of 0.01 throughout the growth of the SOA particles. Based on this comparison, we can conclude that at low RH, the measured depolarisation ratio was due to the physical properties of the α-pinene SOA particles and not a result of window artefacts.

The measured linear depolarisation ratio averaged between 0.01 and 0.1, and the circular depolarisation ratio varied between 0.05 and 0.3 (Figs. 4 ~~, 5~~ and 8). The circular depolarisation ratio was always higher than linear depolarisation ratio and both showed the same trend, i.e. both signals showed the oscillation maxima and minima at same locations. This is a common feature in depolarisation measurements, and has been discussed in previous work by Mishchenko and Hovenier (1995). In theory, the circular depolarisation ratio is more sensitive to small changes; this sensitivity should provide advantages over linear depolarisation. However, in our case the LOD for circular depolarisation ratio was a factor two higher than that for linear depolarisation ratio. Thus, for this instrument, circular depolarisation offered no clear advantage in our measurements.

A depolarisation ratio that is above the LOD and above the background noise in these experiments suggests the presence of aspherical particles. In this case the magnitude of the depolarisation signal depends on the size and shape of the particles. The increase in the depolarisation at the beginning of the runs can be linked with the growth in the particle size, as can be expected from the T-matrix model (Fig. 2). A median particle diameter of 100~~nm~~ nm was sufficient to produce a noise-free depolarisation ratio above the detection threshold; the highest depolarisation ratio was measured for 600~~nm~~ nm particles (Fig. 4). The maximum linear depolarisation ratio varied between 0.05 and 0.1, which corresponds to an aspect ratio of 0.8 to 0.74 according to the T-matrix model for spheroidal particles. The good agreement of the spheroidal model with our measurements support the hypothesised presence of SOA aggregates that grow quasi-spheroidal. Later in the experiments, condensational growth drives the particles to become increasingly spherical, which is also indicated by our measurements, as a slight decrease in the depolarisation ratio as the particle median diameter grew beyond 600~~nm~~ nm.

In the early stages of experiment RUN2_-10C we observed a single mode of growing α-pinene SOA particles (Fig. 4) suggesting that the depolarisation properties of the particles were produced by a single particle population. The narrowness of the size distribution could explain the oscillations that we frequently observed in the depolarisation signal. It should be possible to confirm this conclusion by simulating the scattering properties of the evolving spheroidal particles, but that is beyond the scope of this work and will be addressed in a future study.

As described in ~~section~~ Sect. 3.1, secondary nucleation occurred in some of our experiments, resulting in a bimodal size distribution. Figure 9 shows such a run with two growing modes. The main mode was somewhat wider than in the single-mode experiments, so we do not see clear oscillations in the depolarisation signal. A new narrow mode was nucleated after 15:00 UTC, causing oscillations in the depolarisation signal, as the new mode grew. The measured depolarisation is, therefore, likely due to the net scattering and depolarisation contributions from both of these modes, making the interpretation of the depolarisation properties more challenging. Although the size distribution is not confined to a single size in the bimodal runs, the phase of the new particles was viscous, since the mode was formed before a significant increase in RH. The asphericity of the new mode is also observed in the oscillations that are caused by the newly nucleated narrow mode.

4.4 The atomic oxygen to carbon ratio of the α-pinene SOA

The atomic oxygen to carbon (O~~/~~/C) ratio of SOA particles increases with particle ageing and is related to the hygroscopicity of the particles (Massoli et al., 2010; Duplissy et al., 2011; Lambe et al., 2011). The O~~/~~/C ratio affects the particle ~~hardness~~deliquescence point; in the case of α-pinene SOA particles, ~~the hardness increases~~ we can expect the deliquescence point to be at higher temperatures with increasing O~~/~~/C ratio (Berkemeier et al., 2014). This might affect the particle shape and refractive index variation inside the particle, as higher hardness increases the possibility that the particles remain aspherical and thus induce higher depolarisation signal.

We measured the O~~/~~/C ratio using the HR-ToF-AMS (Aiken et al., 2007, 2008). The measured O~~/~~/C ratios varied from 0.23 to 0.29 with an average value of ~~0.25 ± 0.04~~ 0.25 ± 0.04 (average ± standard deviation). ~~The O/ C ratios decreased slightly with time during each~~ Overall, the O / C stays pretty constant throughout the experiment (Fig. 10). The average O~~/~~/C ratio (below 0.3) is similar to that reported by Pajunoja et al. (2014) of laboratory produced α-pinene SOA particles.

The SOA mass concentration shows a steep increase at the beginning of RUN2_-10C due to the continuous addition of ozone and alpha-pinene to the chamber. At 15:35~~UTC~~ UTC the SOA production rate decreased slightly as the fresh supply of ozone was reduced. After switching off the ozone supply at 20:20~~UTC~~ UTC the formation of SOA was stopped and as a result the SOA concentration decreased due to dilution.

4.5 Measured ~~viscosity-transition-RH~~ viscosity/shape-transition RH as a function of temperature

The depolarisation signal in our experiments showed that the viscous α-pinene SOA particles were non-spherical when the nucleation and growth of the particles occurred at low RH. As the RH increases, the ~~highly~~ viscous SOA particles start to take up water. The water uptake is slow, and proceeds gradually with increasing RH (Mikhailov et al., 2009; Zobrist et al., 2011). This is seen by the relatively slow shape transitions observed as the RH increases (Figs. 4~~and 5~~, 8 and 9). In the aqueous phase, the surface area is minimised to reach an energetically favourable state. The minimisation of the surface area results in shape change from aspherical to spherical. This change was observed in the depolarisation ratio at the end of the low-RH runs, as the depolarisation ratio decreased towards the instrument LOD. We determined the transition RH range from the measurements; the start of the transition was detected when the depolarisation ratio started to decrease significantly. The end of the transition was detected when the depolarisation ratio reached a constant level below the detection threshold (highlighted with grey in Figs. 4, ~~9, 8~~ 8 and 9). The RH value at the time the depolarisation had decreased to a constant, zero level, describes the transition to an optically spherical shape. We label this RH value the ~~viscosity-transition~~ viscosity/shape-transition RH.

Figure 11 summarises the complete RH range, where the viscosity~~transition~~/shape-transition were observed for sub-zero temperatures. At 10~~°C adepolarization~~ °C a depolarisation signal over LOD was not ~~observe~~observed, suggesting that the particles were already in a~~liquid state at~~ liquid or low-viscous state at an RH of 12~~% RH . Generally, two results can be obtained from~~ %. Fig. 11 ~~:~~

~~The viscosity-transition~~ shows that the measured viscosity/shape-transition RH increases with decreasing temperature and ~~the RH range, where the transition occurs becomes wider as the temperature decreases.~~

~~The viscosity-transition RH~~ has near linear dependency ~~of~~ on the temperature. At ~~-10°C the viscosity-transition~~ −10 °C the viscosity/shape-transition occurred at RH around 35~~%~~

~~and at -38°~~ % and at -38 °C the transition was observed at around 80~~% RH. Result (ii) can be linked to the transition timescales, so that at colder temperatures the transition from a solid or semi-solid to liquid will last longer.~~ % RH.

~~The viscosity-transition RH of the SOA particles does not directly provide the glass transition RH, RH_g, since the viscosity transition occurs near the full deliquescence relative humidity (FDRH) , and the glass transition occurs when the relaxation timescales match the experimental timescale . The delay between the RH_g and the FDRH is governed by the competition between the humidification rate and timescale for water diffusion within the particle bulk (Berkemeier et al., 2014)~~ As explained above, our method does not directly measure the change in the viscosity but provides the critical RH, where the water uptake is significantly enhanced and the particles start to relax rapidly due to the change in their viscosity. During this process the viscosity changes of the α-pinene SOA particles are not limited by diffusion on water into the particles as the assumed water diffusion timescales can be expected to be in the order of seconds (Price et al., 2015; Lienhard et al., 2015) . We can now use the observed relaxation time (of the order of 10 minutes) to provide a rough estimate of the viscosity of the α-pinene SOA particles during their viscosity/shape-transition. However, it has to be kept in mind that the particle viscosity and the relaxation timescale are affected by the constant increase in the chamber RH by about 0.5% per minute, which increases the uncertainty of our estimate.

For the estimation of the particle viscosity, we used the method described in Pajunoja et al. (2014) . We can ~~expect that the viscosity transition~~ assume a primary particle size of 400 nm in an SOA aggregate and a surface tension of 35 mN/m (Pajunoja et al., 2014) . With these numbers we get an estimated viscosity of 10^7 Pas. This value describes the viscosity during the viscosity/shape-transition period. Previous studies (e.g. Renbaum-Wolff et al., 2013; Bateman et al., 2014; Kidd et al., 2014; Pajunoja et al., 2014) h studied the viscosity of α-pinene SOA particles at room temperatures. The studies have found that α-pinene SOA particles are generally in liquid state already at RH$>$ 70% (Song et al., 2015) . At colder temperatures we can expect the transition from viscous to liquid state is shifted to ~~somewhat higher RH than the actual RH$_g$ would be. Also it should be noted that the RH$_g$ describes a change in the phase or state of a material at a constant composition, i. e., in a closed system. Our experiments probe the change as composition changes and this likely leads to a continuous variation in the~~ higher RH ~~$_g$. However, the advantage of our setup is that both the particle size and rate of change of RH , correspond roughly to those found in the atmosphere. Moreover, the transition timescales that we observed, 10s of minutes, are relevant to those that we can expect in the atmosphere. Consequently, the viscosity transition RH that we report is relevant for the atmospheric processes and, therefore, can be compared to RH$_g$ in an atmospheric context.~~ (Wang et al., 2014) . As the measured viscosity/shape-transitions generally took place at RH$<$ 70% the comparison with literature would suggest that albeit our SOA particles were spherical, they probably were not in liquid state after the transition. Therefore, our measured viscosity/shape-transition would describe the change in the viscosity within a semi-solid material.

~~We compared~~ The viscosity of α-pinene SOA and their glass-transition as a function of temperature and RH was estimated in the modelling study of (Wang et al., 2014) . Although the authors report an increase in the glass-transition RH with decreasing temperature similar to what we observed in our experiments, the glass-transition RH that they report was always higher than our measured viscosity/shape-transition RH, i.e. we found higher viscosities for the α-pinene SOA particles. Furthermore, we compared our results with the Koop et al. (2011) generic SOA estimate that predicts the glass transition temperature as a function of RH for a broad variety of SOA (Fig. 11). Overall the results agree well with the generic SOA estimate, and significantly reduce the uncertainty in that estimate in the specific case of alpha pinene SOA. Moreover, our results suggest the relationship between the transition RH and the temperature is more linear than predicted by Koop et al. (2011)~~. This may be especially relevant at high RH, where we can expect that the transition might take place at a much higher temperature (around 220 K) than predicted in Koop et al. (2011)~~ , although measurements at colder temperatures are missing.

Our method to detect the ~~viscosity-transition of viscous~~ viscosity/shape-transition of α-pinene SOA is likely limited to laboratory experiments with high number concentrations promoting the formation of non-spherical SOA particle aggregates. ~~Though our limited data do not~~ Although our experimental data is not comprehensive enough to support the hypothesis that SOA particles in the ~~lower~~ troposphere might be non-spherical, we have demonstrated the first non-invasive method to study the viscosity of ~~the SOA particles~~ SOA particles formed by ozonolysis of gaseous α-pinene. Moreover, ~~we observe the viscosity changes on a timescale that is relevant to the atmosphere. This method can be extended to other SOA types and temperature regimes.~~ the transition timescales that we observed, 10 s of minutes, are relevant to those that we can expect in the atmosphere. Therefore, the viscosity/shape-transition RH that we report is relevant for the atmospheric processes. The present study focused on understanding the humidity effect on the viscosity transition temperature of a single SOA component. The method could also be used in future studies to ~~determine the influence of oxidation level or mixing ratio of the SOA precursor to the transition temperature~~study SOA shape transitions of other SOA precursors.

4.6 Atmospheric implications

Atmospheric conditions where SOA is found cover the full range of RH (e.g. Hamed et al., 2011). The observed near-linear dependence of the viscosity~~transition~~ /shape-transition temperature on RH is important for the low temperatures; our results imply that alpha pinene derived SOA particles may remain viscous in the upper troposphere up to ~~very high RH , where previous studies have suggested that they might relax already at lower RH (Koop et al., 2011)~~ an RH of almost 80%. Moreover, the long time required for the ~~phase transition~~ transition from aspherical to spherical suggest that, even though the particles may temporarily be exposed to high RH, they could remain in a viscous state. Hence, this kind of SOA particles may be able to act as IN, especially in the cirrus regime. The IN activity of the same α-pinene SOA particles produced for the present study has been investigated in a parallel study (Ignatius, 2015) using a portable IN counter. They found that, at temperatures below or at the homogeneous freezing limit, the same particles acted as heterogeneous IN in the deposition and immersion modes. However, it is difficult to quantify the effect of the highly viscous SOA on climate; this should be addressed in future studies. Our results were restricted to temperatures above the homogeneous freezing threshold, but, to better understand the phase state of SOA in the cirrus regime, future studies at lower temperatures are needed.

5 Conclusions

The influence of temperature and relative humidity on the ~~viscosity transition~~ viscosity-transition of SOA particles is a subject of considerable uncertainty (Koop et al., 2011). Here, we ~~measured the viscosity transition RH~~ estimated the viscosity of α-pinene SOA at different atmospherically-relevant temperatures ~~using a~~ and relative humidities using a new optical and non-invasive in-situ method. We used near-backscattering depolarisation to measure the asphericity of the SOA particles and ~~the~~ their shape change to spherical ~~at near the full deliquescence relative humidity~~that took place at viscosity of around 10^7 Pas. The relaxation timescales were observed to be ~~10s of minutes -~~ 10 s of minutes – time scales relevant for atmospheric processes. Thus, we conclude that the viscosity~~transition RH provides a~~ /shape-transition RH defined by our method provides a quantity that is directly relevant for glassy transitions of SOA particles in the atmosphere, although the viscosity of the SOA particles cannot be directly determined from our measurements.

We showed that α-pinene SOA particles acquire a non-spherical shape due to coagulation in our chamber experiments. The non-spherical shape persists when the particles are nucleated and grown under low RH. This non-spherical shape is a result of the viscosity of the particles and this viscous state can be detected with depolarisation measurements for SOA particles larger than 100~~nm~~ nm.

We observed ~~the viscositytransition~~ viscosity/shape-transition in six experiments conducted at at four temperatures. We found that ~~the viscositytransition~~ this viscosity/shape-transition temperature depends linearly on RH. This increases the likelihood that α-pinene SOA particles persist in a viscous state at low temperatures, making them potential ice nuclei (IN) in the cirrus cloud regime. Generally, our results improve the understanding of the viscosity ~~transition temperature RH~~ of α-pinene SOA at temperatures above the homogeneous freezing point. The influence of highly viscous SOA on climate should be further assessed in future modelling studies.

Acknowledgements. We would like to thank the two anonymous Referees for their valuable comments. We thank CERN for supporting CLOUD with important technical and financial resources. We thank the CLOUD-TRAIN community and specially all the ITN-students for their help and support. This research has received funding from the Seventh Framework Programme of the European Union (Marie Curie-Networks for Initial Training MC-ITN CLOUD-TRAIN no. ~~316662~~316 662), from Swiss National Science Foundation (SNSF) grant number 200021_140663, from US National Science Foundation Grants AGS-1447056 and AGS-1439551, from Dreyfus Award EP-11-117, from German Federal Ministry of Education and Research BMBF (project no. 01LK1222A and B), from the Davidow Foundation, and from the funding of the German Federal Ministry of Education and Research (BMBF) through the CLOUD12 project.

The article processing charges for this open-access publication were covered by a Research Centre of the Helmholtz Association.

References

Adler, G., Koop, T., Haspel, C., Taraniuk, I., Moise, T., Koren, I., Heiblum, R. H., and Rudich, Y.: Formation of highly porous aerosol particles by atmospheric freeze-drying in ice clouds, P. Natl. Acad. Sci. USA, 110, 20414–20419, doi:10.1073/pnas.1317209110, 2013.

Aiken, A. C., DeCarlo, P. F., and Jimenez, J. L.: Elemental analysis of organic species with electron ionization high-resolution mass spectrometry, Anal. Chem., 79, 8350–8358, 2007.

Aiken, A. C., Decarlo, P. F., Kroll, J. H., Worsnop, D. R., Huffman, J. A., Docherty, K. S., Ulbrich, I. M., Mohr, C., Kimmel, J. R., Sueper, D., Sun, Y., Zhang, Q., Trimborn, A., Northway, M., Ziemann, P. J., Canagaratna, M. R., Onasch, T. B., Alfarra, M. R., Prevot, A. S. H., Dommen, J., Duplissy, J., Metzger, A., Baltensperger, U., and Jimenez, J. L.: O/C and OM/OC ratios of primary, secondary, and ambient organic aerosols with high-resolution time-of-flight aerosol mass spectrometry, Environ. Sci. Technol., 42, 4478–4485, 2008.

Bateman, A. P., Belassein, H., and Martin, S. T.: Impactor apparatus for the study of particle rebound: Relative humidity and capillary forces, Aerosol Sci. Tech., 48, 42–52, 2014.

Berkemeier, T., Shiraiwa, M., Pöschl, U., and Koop, T.: Competition between water uptake and ice nucleation by glassy organic aerosol particles, Atmos. Chem. Phys., 14, 12513–12531, doi:10.5194/acp-14-12513-2014, 2014.

Dal Maso, M., Kulmala, M., Riipinen, I., Wagner, R., Hussein, T., Aalto, P. P., and Lehtinen, K. E.: Formation and growth of fresh atmospheric aerosols: eight years of aerosol size distribution data from SMEAR II, Hyytiala, Finland, Boreal Environ. Res., 10, 323–336, 2005.

Dlugach, J. M. and Mishchenko, M. I.: Scattering properties of heterogeneous mineral particles with absorbing inclusions, J. Quant. Spectrosc. Ra., 162, 89–94, 2015.

Duplissy, J., DeCarlo, P. F., Dommen, J., Alfarra, M. R., Metzger, A., Barmpadimos, I., Prevot, A. S. H., Weingartner, E., Tritscher, T., Gysel, M., Aiken, A. C., Jimenez, J. L., Canagaratna, M. R., Worsnop, D. R., Collins, D. R., Tomlinson, J., and Baltensperger, U.: Relating hygroscopicity and composition of organic aerosol particulate matter, Atmos. Chem. Phys., 11, 1155–1165, doi:10.5194/acp-11-1155-2011, 2011.

Duplissy, J., Merikanto, J., Franchin, A., Tsagkogeorgas, G., Kangasluoma, J., Wimmer, D., Vuollekoski, H., Schobesberger, S., Lehtipalo, K., Flagan, R., Brus, D., Donahue, N. M., Vehkämäki, H., Almeida, J., Amorim, A., Barmet, P., Bianchi, F., Breitenlechner, M., Dunne, E. M., Guida, R., Henschel, H., Junninen, H., Kirkby, J., Kürten, A., Kupc, A., Määttänen, A., Makhmutov, V., Mathot, S., Nieminen, T., Onnela, A., Praplan, A. P., Riccobono, F., Rondo, L., Steiner, G., Tome, A., Walther, H., Baltensperger, U., Carslaw, K. S., Dommen, J., Hansel, A., Petäjä, T., Sipilä, M., Stratmann, F., Vrtala, A., Wagner, P. E., Worsnop, D. R., Curtius, J., and Kulmala, M.: Effect of ions on sulfuric acid-water binary particle formation II: Experimental data and comparison with QC-normalized classical nucleation theory, J. Geophys. Res.-Atmos., 120, doi:10.1002/2015JD023539, 2015.

~~The SOA particles were modelled as prolate spheroids. An ESEM image of the SOA particles sampled from the CLOUD chamber show a spheroidal "egg-like" shape. The shape of the SOA particles in the ESEM images does not necessary resemble the real shape of the particles in the chamber~~

Fahey, D. W., Gao, R.-S., Möhler, O., Saathoff, H., Schiller, C., Ebert, V., Krämer, M., Peter, T., Amarouche, N., Avallone, L. M., Bauer, R., Bozóki, Z., Christensen, L. E., Davis, S. M., Durry, G., Dyroff, C., Herman, R. L., Hunsmann, S., Khaykin, S. M., Mackrodt, P., Meyer, J., Smith, J. B., Spelten, N., Troy, R. F., Vömel, H., Wagner, S., and Wienhold, F. G.: The AquaVIT-1 intercomparison of atmospheric water vapor measurement techniques, Atmos. Meas. Tech., 7, ~~due to sampling conditions. In the~~ 3177–3213, doi:10.5194/amt-7-3177-2014, 2014.

Guenther, A., Hewitt, C. N., Erickson, D., Fall, R., Geron, C., Graedel, T., Harley, P., Klinger, L., Lerdau, M., McKay, W., Pierce, T., Scholes, B., Steinbrecher, R., Tallamraju, R., Taylor, J., and Zimmerman, P.: A global model of natural volatile organic compound emissions, J. Geophys. Res.-Atmos., 100, 8873–8892, 1995.

Hallquist, M., Wenger, J. C., Baltensperger, U., Rudich, Y., Simpson, D., Claeys, M., Dommen, J., Donahue, N. M., George, C., Goldstein, A. H., Hamilton, J. F., Herrmann, H., Hoffmann, T., Iinuma, Y., Jang, M., Jenkin, M. E., Jimenez, J. L., Kiendler-Scharr, A., Maenhaut, W., McFiggans, G., Mentel, Th. F., Monod, A., Prévôt, A. S. H., Seinfeld, J. H., Surratt, J. D., Szmigielski, R., and Wildt, J.: The formation, properties and impact of secondary organic aerosol: current and emerging issues, Atmos. Chem. Phys., 9, 5155–5236, doi:10.5194/acp-9-5155-2009, 2009.

Hamed, A., Korhonen, H., Sihto, S.-L., Joutsensaari, J., Järvinen, H., Petäjä, T., Arnold, F., Nieminen, T., Kulmala, M., Smith, J. N., Lehtinen, K. E. J., and Laaksonen, A.: The role of relative humidity in continental new particle formation, J. Geophys. Res.-Atmos., 116, D03202, doi:10.1029/2010JD014186, 2011.

Hirsikko, A., O'Connor, E. J., Komppula, M., Korhonen, K., Pfüller, A., Giannakaki, E., Wood, C. R., Bauer-Pfundstein, M., Poikonen, A., Karppinen, T., Lonka, H., Kurri, M., Heinonen, J., Moisseev, D., Asmi, E., Aaltonen, V., Nordbo, A., Rodriguez, E., Lihavainen, H., Laaksonen, A., Lehtinen, K. E. J., Laurila, T., Petäjä, T., Kulmala, M., and Viisanen, Y.: Observing wind, aerosol particles, cloud and precipitation: Finland's new ground-based remote-sensing network, Atmos. Meas. Tech., 7, 1351–1375, doi:10.5194/amt-7-1351-2014, 2014.

Hoyle, C. R., Boy, M., Donahue, N. M., Fry, J. L., Glasius, M., Guenther, A., Hallar, A. G., Huff Hartz, K., Petters, M. D., Petäjä, T., Rosenoern, T., and Sullivan, A. P.: A review of the anthropogenic influence on biogenic secondary organic aerosol, Atmos. Chem. Phys., 11, 321–343, doi:10.5194/acp-11-321-2011, 2011.

Hoyle, C. R. and Fuchs, C. and Järvinen, E. and Saathoff, H. and Dias, A. and El Haddad, I. and Gysel, M. and Coburn, S. C. and Tröstl, J. and Bernhammer, A.-K. and Bianchi, F. and Breitenlechner, M. and Corbin, J. C. and Craven, J. and Donahue, N. M. and Duplissy, J. and Ehrhart, S. and Frege, C. and Gordon, H. and Höppel, N. and Heinritzi, M. and Kristensen, T. B. and Molteni, U. and Nichman, L. and Pinterich, T. and Prévôt, A. S. H. and Simon, M. and Slowik, J. G. and Steiner, G. and Tomé, A. and Vogel, A. L. and Volkamer, R. and Wagner, A. C. and

Wagner, R. and Wexler, A. S. and Williamson, C. and Winkler, P. M. and Yan, C. and Amorim, A. and Dommen, J. and Curtius, J. and Gallagher, M. W. and Flagan, R. C. and Hansel, A. and Kirkby, J. and Kulmala, M. and Möhler, O. and Stratmann, F. and Worsnop, D. R. and Baltensperger, U.: Aqueous phase oxidation of sulphur dioxide by ozone in cloud droplets, Atmos. Chem. Phys., 16, 1693–1712, doi:10.5194/acp-16-1693-2016, 2016.

Huang, R.-J., Zhang, Y., Bozzetti, C., Ho, K.-F., Cao, J.-J., Han, Y., Daellenbach, K. R., Slowik, J. G., Platt, S. M., Canonaco, F., Zotter, P., Wolf, R., Pieber, S. M., Bruns, E. A., Crippa, M., Ciarelli, G., Piazzalunga, A., Schwikowski, M., Abbaszade, G., Schnelle-Kreis, J., Zimmermann, R., An, Z., Szidat, S., Baltensperger, U., El Haddad, I., and Prévôt, A. S. H.: High secondary aerosol contribution to particulate pollution during haze events in China, Nature, 514, 218–222, 2014.

Ignatius, K.: Heterogeneous ice nucleation of viscous secondary organic aerosol produced from ozonolysis of alpha-pinene, Atmos. Chem. Phys. Discuss., in preparation, 2015.

Jimenez, J. L., Canagaratna, M. R., Donahue, N. M., Prevot, A. S. H., Zhang, Q., Kroll, J. H., DeCarlo, P. F., Allan, J. D., Coe, H., Ng, N. L., Aiken, A. C., Docherty, K. S., Ulbrich, I. M., Grieshop, A. P., Robinson, A. L., Duplissy, J., Smith, J. D., Wilson, K. R., Lanz, V. A., Hueglin, C., Sun, Y. L., Tian, J., Laaksonen, A., Raatikainen, T., Rautiainen, J., Vaattovaara, P., Ehn, M., Kulmala, M., Tomlinson, J. M., Collins, D. R., Cubison, M. J., E., Dunlea, J., Huffman, J. A., Onasch, T. B., Alfarra, M. R., Williams, P. I., Bower, K., Kondo, Y., Schneider, J., Drewnick, F., Borrmann, S., Weimer, S., Demerjian, K., Salcedo, D., Cottrell, L., Griffin, R., Takami, A., Miyoshi, T., Hatakeyama, S., Shimono, A., Sun, J. Y., Zhang, Y. M., Dzepina, K., Kimmel, J. R., Sueper, D., Jayne, J. T., Herndon, S. C., Trimborn, A. M., Williams, L. R., Wood, E. C., Middlebrook, A. M., Kolb, C. E., Baltensperger, U., and Worsnop, D. R.: Evolution of organic aerosols in the atmosphere, Science, 326, 1525–1529, 2009.

Kim, H., Barkley, B., Paulson, S. E.: Real refractive indices of α-and β-pinene and toluene secondary organic aerosols generated from ozonolysis and photo-oxidation, J. Geophys. Res. Atmos., 115, D24, 2010.

Kidd, C., Perraud, V., Wingen, L. M., Finlayson-Pitts, B. J.: Integrating phase and composition of secondary organic aerosol from the ozonolysis of α-pinene, PNAS., 111, 7552–7557, 2014.

Kirkby, J., Curtius, J., Almeida, J., Dunne, E., Duplissy, J., Ehrhart, S., Franchin, A., Gagné, S., Ickes, L., Kürten, A., et al.: Role of sulphuric acid, ammonia and galactic cosmic rays in atmospheric aerosol nucleation, Nature, 476, 429–433, 2011.

Koop, T., Bookhold, J., Shiraiwa, M., and Pöschl, U.: Glass transition and phase state of organic compounds: dependency on molecular properties and implications for secondary organic aerosols in the atmosphere, Phys. Chem. Chem. Phys., 13, 19238–19255, 2011.

Kulmala, M., Riipinen, I., Sipilä, M., Manninen, H. E., Petäjä, T., Junninen, H., Dal Maso, M., Mordas, G., Mirme, A., Vana, M., Hirsikko, A., Laakso, L., Harrison, R. M., Hanson, I., Leung, C., Lehtinen, K. E. J., and Kerminen, V. M.: Toward direct measurement of atmospheric nucleation, Science, 318, 89–92, 2007.

Kulmala, M., Kontkanen, J., Junninen, H., Lehtipalo, K., Manninen, H. E., Nieminen, T., Petäjä, T., Sipilä, M., Schobesberger, S., Rantala, P., Franchin, A., Jokinen, T., Järvinen, E., Äijälä, M., Kangasluoma, J., Hakala, J., Aalto, P. P., Paasonen, P., Mikkilä, J., Vanhanen, J., Aalto, J., Hakola, H., Makkonen, U., Ruuskanen, T., Mauldin III, R. L., Duplissy, J., Vehkamäki, H., Bäck, J., Kortelainen, A., Riipinen, I., Kurtén, T., Johnston, M. V., Smith, J. N., Ehn, M., Mentel, T. F., Lehtinen, K. E. J., Laaksonen, A., Kerminen, V. M., and Worsnop, D. R.: Direct observations of atmospheric aerosol nucleation, Science, 339, 943–946, 2013.

Laaksonen, A., Kulmala, M., O'Dowd, C. D., Joutsensaari, J., Vaattovaara, P., Mikkonen, S., Lehtinen, K. E. J., Sogacheva, L., Dal Maso, M., Aalto, P., Petäjä, T., Sogachev, A., Yoon, Y. J., Lihavainen, H., Nilsson, D., Facchini, M. C., Cavalli, F., Fuzzi, S., Hoffmann, T., Arnold, F., Hanke, M., Sellegri, K., Umann, B., Junkermann, W., Coe, H., Allan, J. D., Alfarra, M. R., Worsnop, D. R., Riekkola, M. -L., Hyötyläinen, T., and Viisanen, Y.: The role of VOC oxidation products in continental new particle formation, Atmos. Chem. Phys., 8, 2657–2665, doi:10.5194/acp-8-2657-2008, 2008.

Lambe, A. T., Onasch, T. B., Massoli, P., Croasdale, D. R., Wright, J. P., Ahern, A. T., Williams, L. R., Worsnop, D. R., Brune, W. H., and Davidovits, P.: Laboratory studies of the chemical composition and cloud condensation nuclei (CCN) activity of secondary organic aerosol (SOA) and oxidized primary organic aerosol (OPOA), Atmos. Chem. Phys., 11, 8913–8928, doi:10.5194/acp-11-8913-2011, 2011.

Li, X., Taflove, A., and Backman, V.: Quantitative analysis of depolarization of backscattered light by stochastically inhomogeneous dielectric particles, Opt. Lett., 30, 902–904, 2005.

Lienhard, D. M., Huisman, A. J., Krieger, U. K., Rudich, Y., Marcolli, C., Luo, B. P., Bones, D. L., Reid, J. P., Lambe, A. T., Canagaratna, M. R. and et al.: Viscous organic aerosol particles in the upper troposphere: diffusivity-controlled water uptake and ice nucleation?, Atmos. Chem. Phys., 15, 13599–13613, 2015.

Massoli, P., Lambe, A., Ahern, A., Williams, L., Ehn, M., Mikkilä, J., Canagaratna, M., Brune, W., Onasch, T., Jayne, J., Petäjä, T., Kulmala, M., Laaksonen, A., Kolb, C. E., Davidovits, P., and Worsnop, D. R.: Relationship between aerosol oxidation level and hygroscopic properties of laboratory generated secondary organic aerosol (SOA) particles, Geophys. Res. Lett., 37, L24801, doi:10.1029/2010GL045258, 2010.

Mikhailov, E., Vlasenko, S., Martin, S. T., Koop, T., and Pöschl, U.: Amorphous and crystalline aerosol particles interacting with water vapor: conceptual framework and experimental evidence for restructuring, phase transitions and kinetic limitations, Atmos. Chem. Phys., 9, 9491–9522, doi:10.5194/acp-9-9491-2009, 2009.

Mishchenko, M. and Hovenier, J.: Depolarization of light backscattered by randomly oriented nonspherical particles, Opt. Lett., 20, 1356–1358, 1995.

Mishchenko, M., Travis, L., and Mackowski, D.: T-matrix ~~notation the aspect ratio (AR) is determined as the relation between the equatorial radius to the polar radius (a~~ computations of light scattering by nonspherical particles: a review, J. Quant. Spectrosc. Ra., 55, 535–575, 1996.

Murray, B. J., Wilson, T. W., Dobbie, S., Cui, Z., Al-Jumur, S. M., Möhler, O., Schnaiter, M., Wagner, R., Benz, S., Niemand, M., Saathoff, H., Ebert, V., Wagner, S., and Kärcher, B.: Heterogeneous nucleation of ice particles on glassy aerosols under cirrus conditions, Nat. Geosci., 3, 233–237, 2010.

Naumann, K.-H.: COSIMA – a computer program simulating the dynamics of fractal aerosols, J. Aerosol Sci., 34, 1371–1397, 2003.

Nel, A.: Air pollution-related illness: effects of particles, Science, 308, 804–806, doi:10.1126/science.1108752, 2005.

Pajunoja, A., Malila, J., Hao, L., Joutsensaari, J., Lehtinen, K. E., and Virtanen, A.: Estimating the viscosity range of SOA particles based on their coalescence time, Aerosol Sci. Tech., 48, i–iv, 2014.

Pajunoja, A., Lambe, A. T., Hakala, J., Rastak, N., Cummings, M. J., Brogan, J. F., Hao, L., Paramonov, M., Hong, J., Prisle, N. L., Malila, J., Romakkaniemi, S., Lehtinen, K. E. J., Laaksonen, A., Kulmala, M., Massoli, P., Onasch, T. B., Donahue, N. M., Riipinen, I., Davidovits, P., Worsnop, D. R., Petäjä, T., and Virtanen, A.: Adsorptive uptake of water by semisolid secondary organic aerosols, Geophys. Res. Lett., 42, 3063–3068, 2015.

Price, H. C., Mattsson, J., Zhang, Y., Bertram, A. K., Davies, J. F., Grayson, J. W., Martin, S. T., O'Sullivan, D., Reid, J. P., Rickards, A. MJ. and et al.: Water diffusion in atmospherically relevant α-pinene secondary organic material, Chemical Science, 6, 4876–4883, 2015.

Redmond, H., Thompson, J. E.: Evaluation of a quantitative structure–property relationship (QSPR) for predicting mid-visible refractive index of secondary organic aerosol (SOA), Phys. Chem. Chem. Phys., 13, 6872–6882, 2011.

Renbaum-Wolff, L., Grayson, J. W., Bateman, A. P., Kuwata, M., Sellier, M., Murray, B. J., Shilling, J. E., Martin, S. T., and Bertram, A. K.: Viscosity of α-pinene secondary organic material and implications for particle growth and reactivity, P. Natl. Acad. Sci. USA, 110, 8014–8019, doi:10.1073/pnas.1219548110, 2013.

Riccobono, F., Schobesberger, S., Scott, C. E., Dommen, J., Ortega, I. K., Rondo, L., Almeida, J., Amorim, A., Bianchi, F., Breitenlechner, M., et al.: Oxidation products of biogenic emissions contribute to nucleation of atmospheric particles, Science, 344, 717–721, 2014.

Riipinen, I., Yli-Juuti, T., Pierce, J. R., Petäjä, T., Worsnop, D. R., Kulmala, M., and Donahue, N. M.: The contribution of organics to atmospheric nanoparticle growth, Nat. Geosci., 5, 453–458, 2012.

Sakai, T., Nagai, T., Zaizen, Y., and Mano, Y.: Backscattering linear depolarization ratio measurements of mineral, sea-salt, and ammonium sulfate particles simulated in a laboratory chamber, Appl. Optics, 49, 4441–4449, 2010.

Sassen, K.: The polarization lidar technique for cloud research: A review and current assessment, B. Am. Meteorol. Soc., 72, 1848–1866, 1991.

Saukko, E., Lambe, A. T., Massoli, P., Koop, T., Wright, J. P., Croasdale, D. R., Pedernera, D. A., Onasch, T. B., Laaksonen, A., Davidovits, P., Worsnop, D. R., and Virtanen, A.: Humidity-dependent phase state of SOA particles from biogenic and anthropogenic precursors, Atmos. Chem. Phys., 12, 7517–7529, doi:10.5194/acp-12-7517-2012, 2012.

Schill, G. P., De Haan, D. O., and Tolbert, M. A.: Heterogeneous ice nucleation on simulated secondary organic aerosol, Environ. Sci. Technol., 48, 1675–1682, 2014.

Schnaiter, M., Linke, C., Möhler, O., Naumann, K.-H., Saathoff, H., Wagner, R., Schurath, U., and Wehner, B.: Absorption amplification of black carbon internally mixed with secondary organic aerosol, J. Geophys. Res.-Atmos., 110, D19204, doi:10.1029/2005JD006046, 2005.

Schnaiter, M., Büttner, S., Möhler, O., Skrotzki, J., Vragel, M., and Wagner, R.: Influence of particle size and shape on the backscattering linear depolarisation ratio of small ice crystals – cloud chamber measurements in the context of contrail and cirrus microphysics, Atmos. Chem. Phys., 12, 10465–10484, doi:10.5194/acp-12-10465-2012, 2012.

Schnitzhofer, R., Metzger, A., Breitenlechner, M., Jud, W., Heinritzi, M., De Menezes, L.-P., Duplissy, J., Guida, R., Haider, S., Kirkby, J., Mathot, S., Minginette, P., Onnela, A., Walther, H., Wasem, A., Hansel, A., and the CLOUD Team: Characterisation of organic contaminants in the CLOUD chamber at CERN, Atmos. Meas. Tech., 7, 2159–2168, doi:10.5194/amt-7-2159-2014, 2014.

Shiraiwa, M., Ammann, M., Koop, T., and Pöschl, U.: Gas uptake and chemical aging of semisolid organic aerosol particles, P. Natl. Acad. Sci. USA, 108, 11003–11008, 2011.

Song, M., Liu, P.F., Hanna, S.J., Li, Y.J., Martin, S.T., Bertram, A.K.: Relative humidity-dependent viscosities of isoprene-derived secondary organic material and atmospheric implications for isoprene-dominant forests, Atmos. Chem. Phys., 15, 5145–5159, 2015.

Swietlicki, E., HANSSON, H.-C., Hämeri, K., Svenningsson, B., Massling, A., McFiggans, G., McMurry, P., Petäjä, T., Tunved, P., Gysel, M., Topping, D. Weingartner, E., Baltensperger, U., Rissler, J., Wiedensohler, A., and Kulmala, M.: Hygroscopic properties of submicrometer atmospheric aerosol particles measured with H-TDMA instruments in various environments – a review, Tellus B, 60, 432–469, 2008.

Tunved, P., Hansson, H.-C., Kerminen, V.-M., Ström, J., Dal Maso, M., Lihavainen, H., Viisanen, Y., Aalto, P., Komppula, M., and Kulmala, M.: High natural aerosol loading over boreal forests, Science, 312, 261–263, 2006.

Virtanen, A., Joutsensaari, J., Koop, T., Kannosto, J., Yli-Pirilä, P., Leskinen, J., Mäkelä, J. M., Holopainen, J. K., Pöschl, U., Kulmala, M., Worsnop, D. R., and Laaksonen, A.: An amorphous solid state of biogenic secondary organic aerosol particles, Nature, 467, 824–827, 2010.

Virtanen, A., Kannosto, J., Kuuluvainen, H., Arffman, A., Joutsensaari, J., Saukko, E., Hao, L., Yli-Pirilä, P., Tiitta, P., Holopainen, J. K., Keskinen, J., Worsnop, D. R., Smith, J. N., and Laaksonen, A.: Bounce behavior of freshly nucleated biogenic secondary organic aerosol particles, Atmos. Chem. Phys., 11, 8759–8766, doi:10.5194/acp-11-8759-2011, 2011.

Voigtländer, J., Duplissy, J., Rondo, L., Kürten, A., and Stratmann, F.: Numerical simulations of mixing conditions and aerosol dynamics in the CERN CLOUD chamber, Atmos. Chem. Phys., 12, 2205–2214, doi:10.5194/acp-12-2205-2012, 2012.

Wagner, R., Möhler, O., Saathoff, H., Schnaiter, M., Skrotzki, J., Leisner, T., Wilson, T. W., Malkin, T. L., and Murray, B. J.: Ice cloud processing of ultra-viscous/~~b)~~ glassy aerosol particles leads to enhanced ice nucleation ability, Atmos. Chem. Phys., 12, 8589–8610, doi:10.5194/acp-12-8589-2012, 2012.

Wang, B., Lambe, A. T., Massoli, P., Onasch, T. B., Davidovits, P., Worsnop, D. R., and Knopf, D. A.: The deposition ice nucleation and immersion freezing potential of amorphous secondary organic aerosol: pathways for ice and mixed-phase cloud formation, J. Geophys. Res.-Atmos., 117, D16209, doi:10.1029/2012JD018063, 2012.

Wang, B., O'Brien, R. E., Kelly, S. T., Shilling, J. E., Moffet, R. C., Gilles, M. K., and Laskin,. A.: Reactivity of liquid and semisolid secondary organic carbon with chloride and nitrate in atmospheric aerosols, J. Phys. Chem. A., 119, 4498–4508, 2014.

Wilson, T. W., Murray, B. J., Wagner, R., Möhler, O., Saathoff, H., Schnaiter, M., Skrotzki, J., Price, H. C., Malkin, T. L., Dobbie, S., and Al-Jumur, S. M. R. K.: Glassy aerosols with a range of compositions nucleate ice heterogeneously at cirrus temperatures, Atmos. Chem. Phys., 12, 8611–8632, doi:10.5194/acp-12-8611-2012, 2012.

Zhang, Y., Sanchez, M. S., Douet, C., Wang, Y., Bateman, A. P., Gong, Z., Kuwata, M., Renbaum-Wolff, L., Sato, B. B., Liu, P. F., Bertram, A. K., Geiger, F. M., and Martin, S. T.: Changing shapes and implied viscosities of suspended submicron particles, Atmos. Chem. Phys., 15, 7819–7829, doi:10.5194/acp-15-7819-2015, 2015.

Zobrist, B., Marcolli, C., Pedernera, D. A., and Koop, T.: Do atmospheric aerosols form glasses?, Atmos. Chem. Phys., 8, 5221–5244, doi:10.5194/acp-8-5221-2008, 2008.

Zobrist, B., Soonsin, V., Luo, B. P., Krieger, U. K., Marcolli, C., Peter, T., and Koop, T.: Ultra-slow water diffusion in aqueous sucrose glasses, Phys. Chem. Chem. Phys., 13, 3514–3526, 2011.

Table 1. Experiment list with experiment run number, starting temperature, relative humidity at the beginning, particle size before transition started and ~~is thus < 1~~ measured relative humidity range for ~~prolate spheroids~~the viscosity transition.

Run	CLOUD run number	T [°C]	Start RH [%]	Transition mode mean diameter [nm]	Viscosity transition RH [%]
RUN_10C	CLOUD8 1313	10	12	no transition	no transition
RUN1_-10C	CLOUD8 1314	-10	12	560	23–35
RUN2_-10C	CLOUD9 1511	-10	12	880	31–36
RUN1_-20C	CLOUD9 1512	-20	10	500, 850[2]	44–49
REF_-20C	CLOUD9 1513	-20	60[1]	no transition	no transition
RUN2_-20C	CLOUD9 1514	-20	4	1000	41–45
RUN_-30C	CLOUD9 1515	-30	2	500, 850[2]	55–62
RUN_-38C	CLOUD9 1516	-38	5	630	69–79

[1] RH varied between 60 and 70 %.

[2] More than one mode present.

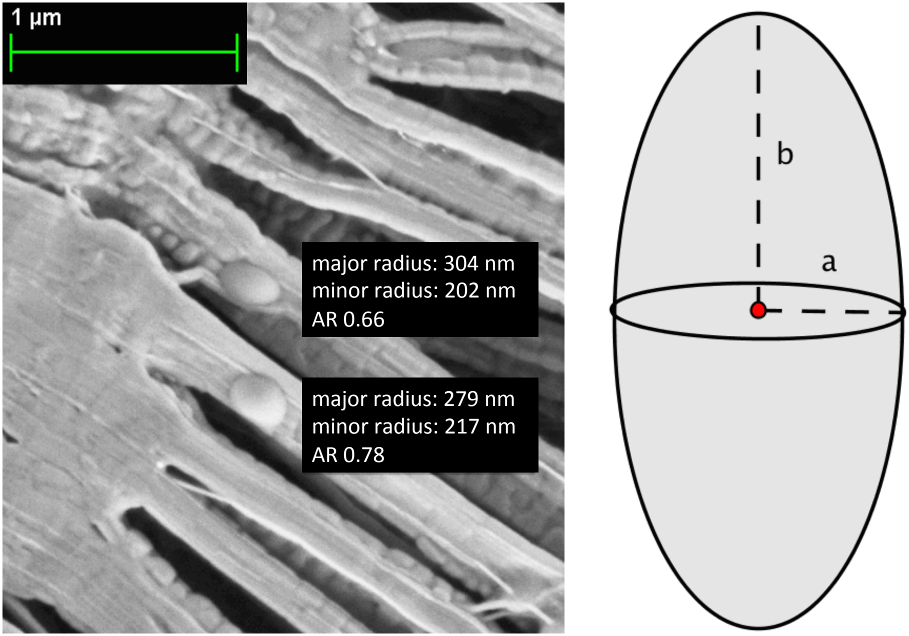

Figure 1. The SOA particles were modelled as prolate spheroids. An ESEM image of the SOA particles sampled from the CLOUD chamber show a spheroidal “egg-like” shape. The shape of the SOA particles in the ESEM images does not necessary resemble the real shape of the particles in the chamber, due to sampling conditions. In the T-matrix notation the aspect ratio (AR) is determined as the relation between the equatorial radius to the polar radius (a / b) and is thus < 1 for prolate spheroids.

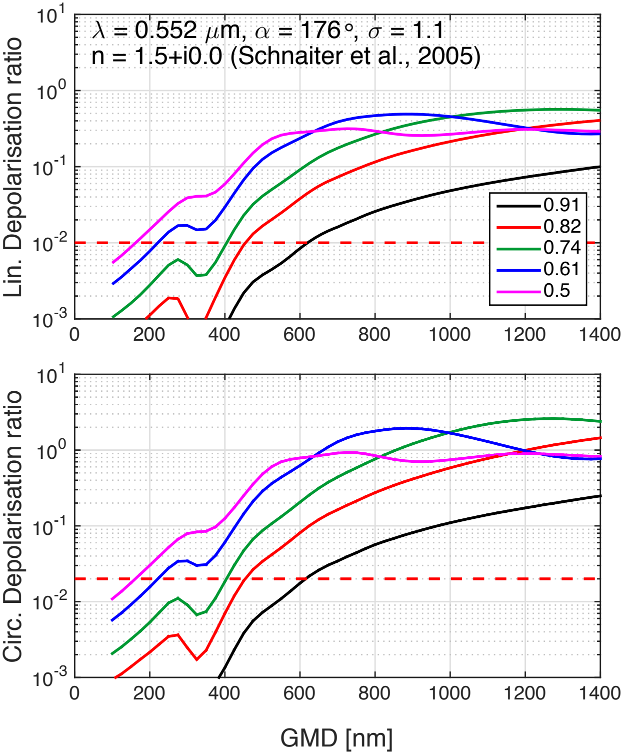

Figure 2. To plan the experiment, the expected linear and circular depolarisation ratios were modelled with the T-matrix model assuming a spheroidal shape. A narrow particle size distribution with a constant GSD of 1.1 was used in the model and the GMD of the particles was varied from 0 to 1400~~nm~~ nm (~~x-axis~~x axis). The calculation was made for five spheroidal shapes with aspect ratios ranging from 0.91 to 0.5. The detection thresholds of the SIMONE-Junior instrument (1~~%~~ % for linear depolarisation and 2~~%~~ % for circular) are indicated as dashed red horizontal lines. The modelling study indicates that the SOA particles need to be grown past 600~~nm~~ nm to produce a detectable depolarisation ratio at aspect ratios up to 0.91.

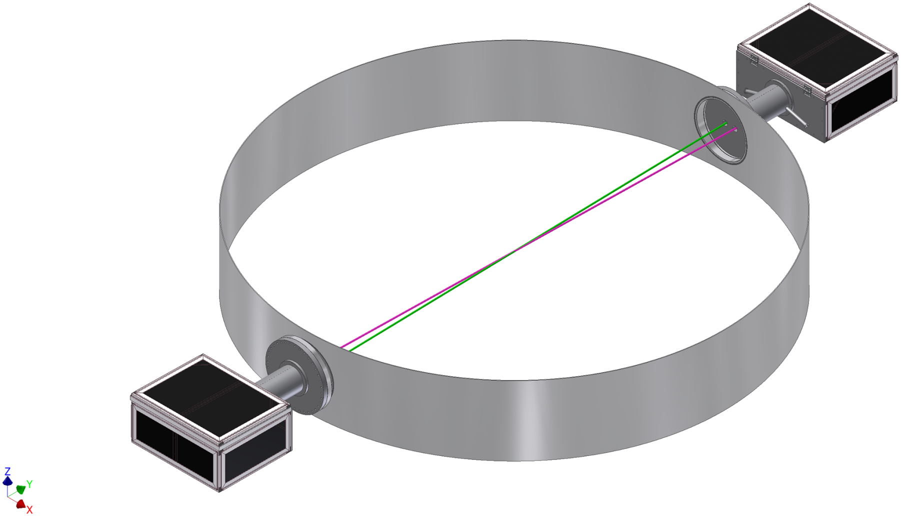

Figure 3. The SIMONE setup at the CERN CLOUD chamber. The instrument consists of two boxes facing each other. One box houses the laser production and the backward scattered light detector and the other box houses the forward scattered light detector and a beam dump. The green line illustrates the path of the laser beam, which crosses the field of view (purple line) of the detection optics. The overlap region defines a detection volume of a few cubic centimetres volume in the centre of the chamber.

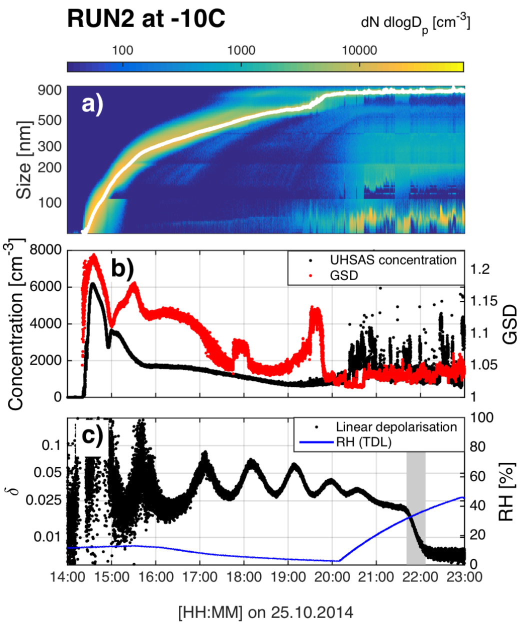

Figure 4. Overview of RUN2 at ~~10°~~ −10 °C. The particle size distribution and the GMD from a log-normal fit are shown in panel ~~A~~(a). Panel ~~B~~ (b) shows the total concentration measured with the UHSAS (with 56~~nm~~ nm cutoff) and the GSD determined from a log-normal fit. Panel ~~C~~ (c) shows the linear depolarisation ratio and RH. The RH was kept low during the growth of the SOA particles, allowing them to remain in a viscous state. The RH was raised after about 20:15 UTC in order to measure its value at the particle phase transition from highly viscous to low viscosity state. The gradual phase transition began at 21:41 UTC and is indicated by the grey area in panel ~~C~~(c). The top and middle panels show further particle nucleation starting around 19:00 UTC; these particles remained relatively small and did not affect the measurement.

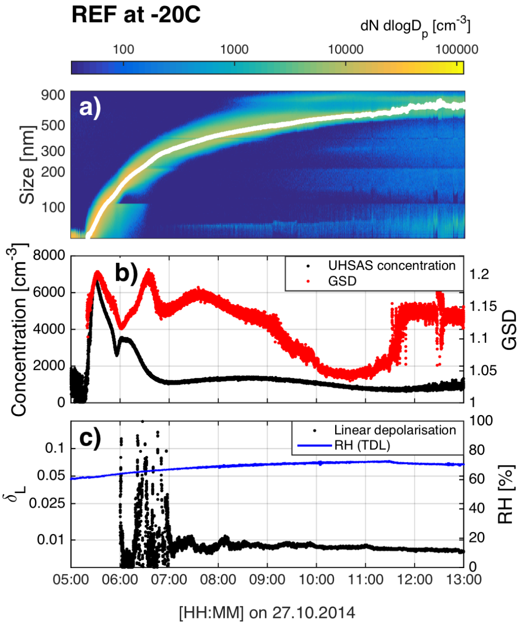

Figure 5. Overview of the reference run at ~~-20°~~ −20 °C. As for ~~figure~~ Fig. 4, panel ~~A~~ **(a)** shows the particle size distribution and the GMD from a log-normal fit. Panel ~~B~~ **(b)** shows the total concentration measured with the UHSAS (with 56~~nm~~ nm cutoff) and the GSD determined from a log-normal fit. Panel ~~C~~ **(c)** shows the time-development of the linear depolarisation ratio and the RH. During the reference run the RH was kept over 60~~%~~ % during the growth of the SOA particles to ensure that they remained in low viscous state during growth. ~~The~~ At the beginning of the growth (6:00-7:00) the SOA particles were too small to efficiently scatter light and the signal shown in panel **(c)** at that time is mostly noise. After the particles were larger than 100 nm, the linear depolarisation ratio stayed below the detection threshold~~during the entire experiment~~, indicating a low viscous state of the particles and verifying the absence of measurement artifacts.

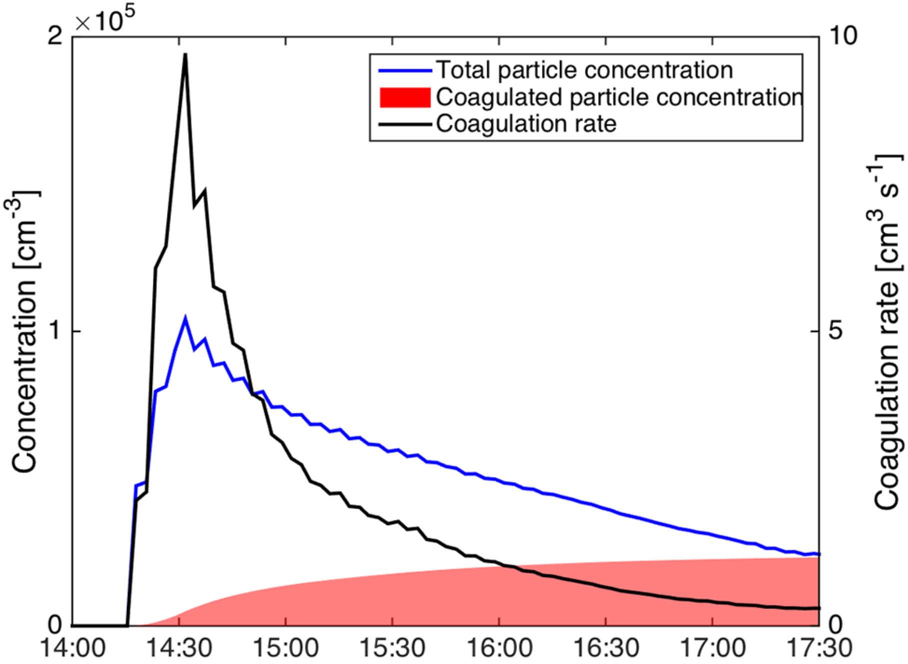

Figure 6. COSIMA model results for the coagulation rate of the SOA particles during experiment RUN2 at ~~-10°~~ −10 °C. The particle number concentration was integrated from the SMPS measurements between 20 ~~nm~~ and 500~~nm~~ nm.

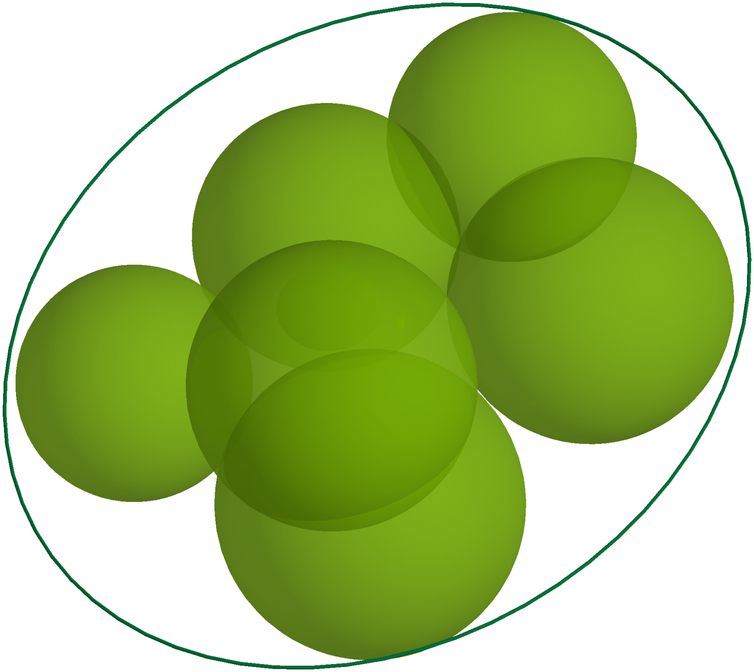

Figure 7. The SOA particles form aggregates at the early stage of their growth. After the coagulation rate has slowed, the aggregates grow by vapour condensation to form non-spherical particles. The number of the single SOA particles in the aggregate is illustrative and does not necessary describe the real aggregates in the CLOUD chamber.

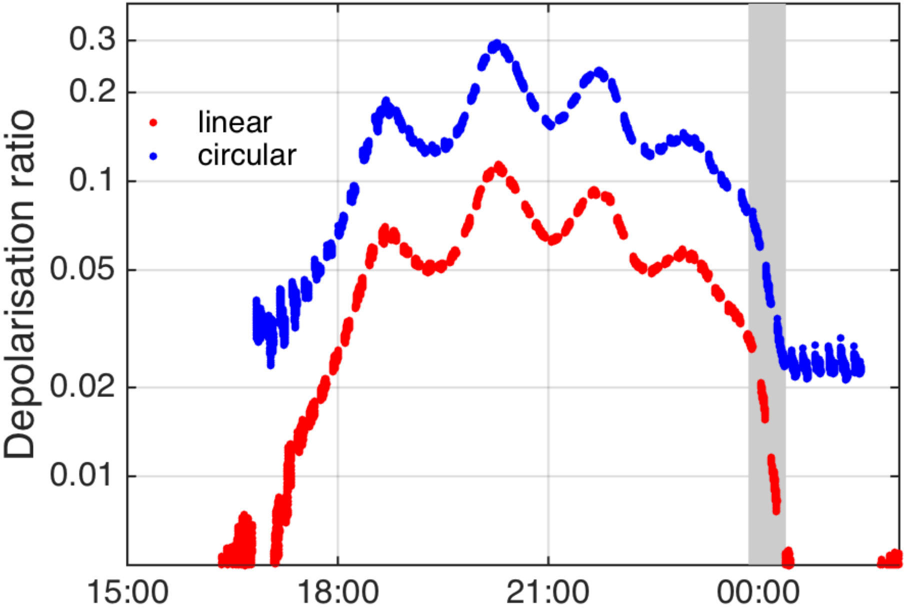

Figure 8. An example of alternating measurements of the linear and the circular depolarisation ratios during RUN_-30C. Both depolarisation ratios show oscillations with consistent minima and maxima. The shape transition is ~~is~~ indicated by the grey area.

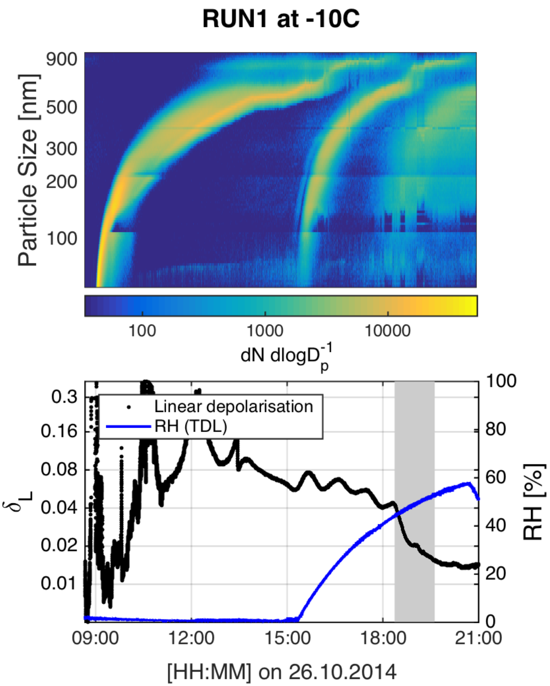

Figure 9. An example of a run with two growing SOA particle modes. The primary mode nucleated around 09:00 UTC and reached a median size of 600~~nm~~ nm around 15:00 UTC, when a second nucleation burst occurred. The new narrow mode produced the oscillations seen in the depolarisation ratio after 15:00 UTC. The main mode was too wide and did not cause oscillations. These particles exhibited a phase transition starting around 18:25 UTC. The noise in the depolarisation signal at the start of the experiment is caused by low signal in the backward detectors.

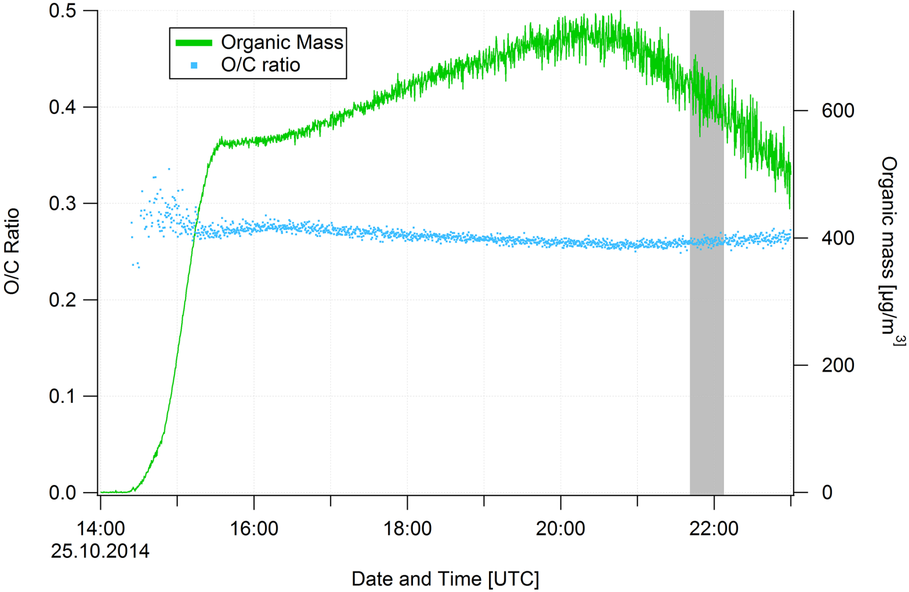

Figure 10. SOA mass concentration (green trace) and ~~O/C~~ O/C ratio of the SOA particles (blue points) measured with the HR-ToF AMS for RUN1_-10C. The grey highlighted area represents the phase transition. The mass concentration represents SOA formed via alpha-pinene ozonolysis; ozone was first added to the chamber during the period of steep growth at the beginning of the experiment. The decrease in SOA concentration towards the end of the experiment was due to dilution. The ~~O/C~~ O/C ratio stayed almost constant throughout the experiment.

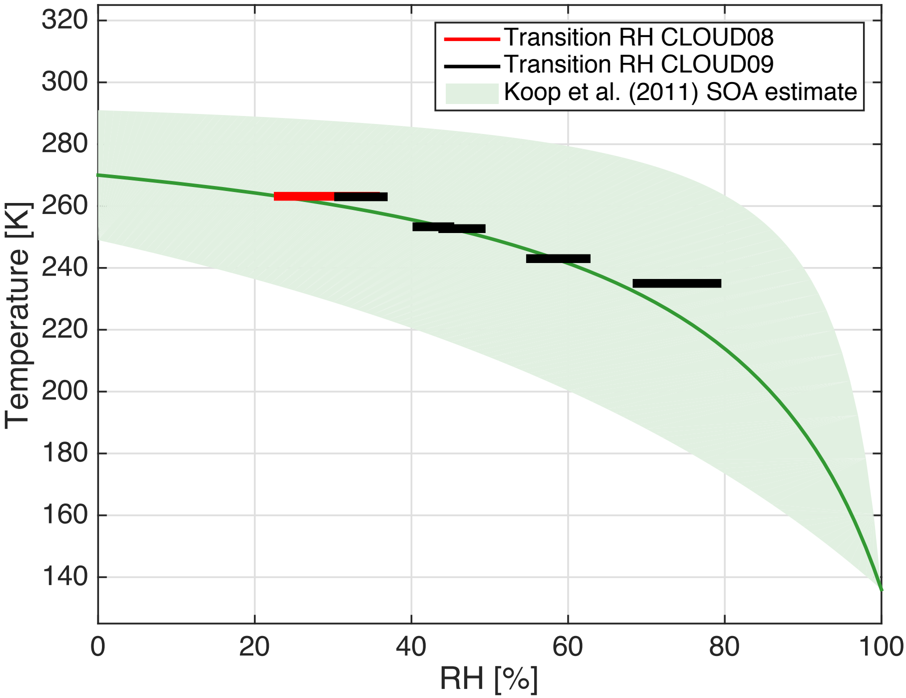
Transition RH CLOUD08
Transition RH CLOUD09
Koop et al. (2011) SOA estimate
Temperature [K]
320
300
280
260
240
220
200
180
160
140
RH [%]
0
20
40
60
80
100

Figure 11. Transition RH at different temperatures. The horizontal lines show the RH range for the transition and the the width of the lines represent the temperature uncertainty of 2~~K~~ K. The green curve is the generic SOA estimate from Koop et al. (2011) and the shaded area represents the upper and lower boundary for the estimate.

~~Experiment list with experiment run number, starting temperature, relative humidity at the beginning, particle size before transition started and measured relative humidity range for the viscosity transition Run CLOUD run number T °CStart RH %Transition mode mean diameter nmViscosity transition RH %0.5exRUNCLOUD8 1313 10 12 no transition no transition RUN1-10C CLOUD8 1314 -10 12 560 23-35 RUN2-10C CLOUD9 1511 -10 12 880 31-36 RUN1-20C CLOUD9 1512 -20 10 500, 850[2] 44-49 REF-20C CLOUD9 1513 -20 60[1] no transition no transition RUN2-20C CLOUD9 1514 -20 4 1000 41-45 RUN-30C CLOUD9 1515 -30 2 500, 850[2] 55-62RUN-38C CLOUD9 1516 -38 5 630 69-79 1ex~~